

TabTreeFormer: Tabular Data Generation Using Hybrid Tree-Transformer

Jiayu Li^{1,2} Bingyin Zhao^{1,2} Zilong Zhao^{1,2}
 Uzair Javaid² Kevin Yee² Biplab Sikdar¹

¹ National University of Singapore, Singapore ² Betterdata AI, Singapore

{li.jiayu,bingyiz,z.zhao,bsikdar}@nus.edu.sg {uzair,kevin}@betterdata.ai

Abstract

Transformers have shown impressive results in tabular data generation. However, they lack domain-specific inductive biases which are critical for preserving the intrinsic characteristics of tabular data. They also suffer from poor scalability and efficiency due to quadratic computational complexity. In this paper, we propose TabTreeFormer, a hybrid transformer architecture that integrates inductive biases of tree-based models (e.g., non-smoothness and non-rotational invariance) to effectively handle the discrete and weakly correlated features in tabular datasets. To improve numerical fidelity and capture multimodal distributions, we introduce a novel tokenizer that learns token sequences based on the complexity of tabular values. This reduces vocabulary size and sequence length, yielding more compact and efficient representations without sacrificing performance. We evaluate TabTreeFormer on nine diverse datasets, benchmarking against eight generative models. We show that TabTreeFormer consistently outperforms baselines in utility, fidelity, and privacy metrics with competitive efficiency. Notably, in scenarios prioritizing data utility over privacy and efficiency, the best variant of TabTreeFormer delivers a 44% performance gain relative to its baseline variant. Our code is available at: <https://anonymous.4open.science/r/tabtreeformer-9585>.

1 Introduction

Tabular data is a prevalent data modality in real-world applications (e.g., healthcare [12], financial services [3], etc.), yet are heavily under-exploited due to privacy concerns [16]. Fortunately, synthetic data offers an alternative to the utilization of tabular data by modeling the characteristics of real data and reducing the risk of data breach [45], thus drawing considerable attention in recent years.

State-of-the-art (SOTA) research shows that transformers such as autoregressive transformers [5], masked transformers [22], and diffusion models with transformers [65] have achieved impressive performance in tabular data generation, allowing synthetic data to empower a variety of fields [24, 3]. However, unlike the application of transformers in other research areas such as computer vision [15] and natural language processing [58], existing transformer models for synthetic tabular data often overlook domain-specific priors (i.e., inductive biases). For example, CvT [63] introduces convolutional embedding and projection to transformers to boost vision performances, and Preprint. Under review.

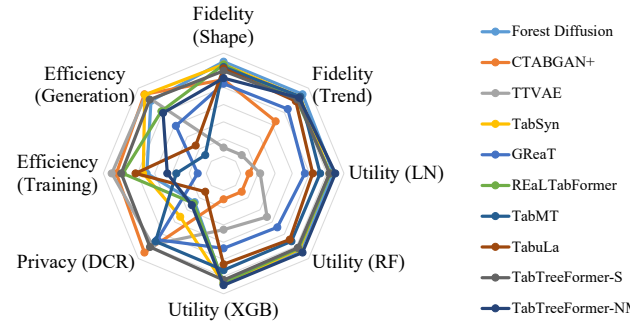


Figure 1: Performance comparison of TabTreeFormer (Ours) with SOTA tabular generative models in utility, fidelity, privacy, and efficiency metrics. TabTreeFormer-S achieves the best balance as the only big near-regular octagon, and TabTreeFormer-NM achieves the best utility.

Transformer-XL [11] introduces segment-level recurrence to transformers to capture longer-term dependencies. While vision and language models have enjoyed the performance boost introduced by domain-specific priors, less exploration has been conducted to leverage them in tabular generative transformers. Moreover, transformers suffer from poor scalability due to quadratic computational complexity. This raises two interesting questions:

1. What inductive biases are beneficial to the quality of synthetically generated tabular data?
2. How can one exploit these inductive biases to improve the generative transformer?

To answer the questions, we propose TabTreeFormer, a hybrid transformer incorporating a tree-based model and a novel tokenizer to handle tabular-specific inductive biases. We also leverage the limited per-dimension semantic meaning (i.e., each dimension corresponds to at most one feature) of typical tabular data to enable a significant reduction in model size with our tokenizer design.

Tree-based models excel at tabular classification and regression tasks [53, 19], which is attributed to their inductive biases that can capture tabular characteristics such as *non-smoothness* and potentially *low-correlation* [21]. Non-smoothness is due to the existence of discrete features and non-smooth relations between discrete and/or continuous features. Trees effectively model these by learning piecewise constant functions, unlike neural networks that typically learn smoother, low-frequency functions [49]. Low-correlated features, often uninformative, contribute minimally to downstream tasks such as classification and regression. Due to the non-rotationally invariant nature of tree-based models [42], trees are more robust against low-correlated features, while neural networks are biased towards stronger correlations everywhere. Inspired by the success of tree models on tabular tasks, we propose to employ such priors to facilitate the performance on tabular generative tasks.

However, tree models do not inherently capture *multimodal distributions* in continuous features (i.e., features whose probability density functions have multiple modes or peaks). This limitation poses a significant challenge for tabular generative modeling. Inspired by [64] that addresses this issue via multimodal decomposition, we propose dual-quantization tokenization for transformers. The first quantization uses K-Means clustering [35] to model multimodal distributions, while the second employs a separate quantile-based quantization to achieve more precise representation of numerical values. Unlike typical word tokens, quantized tokens possess ordinal relationships. To effectively capture these relationships, we design and implement custom embeddings and loss functions.

Our contributions are summarized as follows:

- To the best of our knowledge, we are first to introduce tabular-specific inductive biases to transformers with a tree-based model for improving tabular generative models.
- We introduce a dual-quantization tokenizer for transformers with ordinal-aware embeddings and loss functions to model multimodal continuous features and integrate effectively with transformers for generating high-quality synthetic data.
- Compared to eight baselines across nine datasets, TabTreeFormer achieves an outstanding balance in quality, privacy, and efficiency, as shown in Fig. 1. It also achieves up to 54% and 44% gain over the best deep and general baselines respectively, when prioritizing utility over other metrics.

2 Related Works

2.1 Tabular Data Generation

Early works on tabular data generation use MLPs and CNNs as backbone architectures with GAN and VAE as generation methods [44, 64, 67, 69]. Recent works now use transformers with auto-regression, masked modeling, and diffusion as generative paradigms [5, 65, 22]. For example, TabMT [22] employs a masked transformer with ordered embedding and achieves good utility and scalability in downstream tasks. TabSyn [65] encodes tabular data into a latent space and generates tabular data using a diffusion model, demonstrating impressive fidelity and utility. Despite their enhanced performance, they overlook inductive biases to capture non-smoothness and low-correlated features that are crucial to preserving the intrinsic characteristics of tabular data. Moreover, Xu et al. [64] highlight that capturing multimodal distribution in continuous features is a critical challenge for tabular generative models. CTGAN [64] uses variational Gaussian mixture model [4] to decompose multimodal values, while TabDiff [51] introduces a multimodal stochastic sampler. In this paper, we propose a tokenizer that models the multimodal distribution and injects this prior into an auto-regressive transformer for improved tabular data generation.

2.2 Tree-based Models for Tabular Data

Tree-based models like XGBoost [10], LightGBM [31], and CatBoost [46] dominate tabular tasks due to their strong inductive biases, enabling high predictive performance, efficiency, and scalability. While transformer-based models [29, 2, 27] show promise, they often underperform due to lack of such biases [53, 19]. Tree-based generative models [61, 38, 30], though efficient, struggle with synthetic data quality or suffer from privacy leakage risks. In this paper, we bridge the gap by combining tree-based priors with transformers to inject tabular-specific inductive bias and enhance tabular generative performance.

2.3 Tabular Tokenizers

Transformers require a tokenizer to convert tabular data into suitable input tokens. Some methods map data to a continuous space by redesigning embedding layers [2, 20, 65], while others tokenize into discrete sequences with minimal embedding changes [5, 55, 22, 68], which align better with NLP practices. In this paper, we adopt the latter to optimize and simplify tabular tokenization. This approach converts continuous values to discrete tokens, which have ordinal relations, such that the greatness of the token IDs can be compared. To capture this relation, two aspects where a model can be modified to cater for the ordinal token space are: i) embedding (input, also output for causal language models) and ii) loss (output).

Ordinal Embedding. One of the most well-known continuous embedding methods is the positional embedding based on trigonometric functions [58] that has been adopted for ordinal tokens [41]. However, their periodic nature is better suited for language positions than general ordinal data. Other methods often rely on non-ordinal embeddings [34, 22] or require high-precision raw values [20, 22]. We propose a function-based ordinal embedding that sidesteps both demands.

Ordinal Loss. Prior work on ordinal regression often targets a small number of classes [43, 28, 8, 52], or modifies cross-entropy loss to account for token distances [14, 40, 9, 66]. Building on core ideas from prior work, we propose a custom loss tailored to our setting.

3 TabTreeFormer

Our goal is to improve generative modeling of tabular data by introducing domain-specific inductive biases. Let \mathbf{X} be the training dataset with n rows, m_d discrete, and m_c continuous features. To generate synthetic tabular data \mathbf{X}' similar to \mathbf{X} , we propose TabTreeFormer, a model composed of three components: a tree-based model, a tokenizer, and a transformer, as shown in Fig. 2. The tree model encodes tabular-specific inductive biases; the tokenizer captures multimodal distributions while reducing vocabulary and sequence length; and the transformer learns priors from both to generate high-quality synthetic data. More details on training and generation are provided in Appendix A.1.

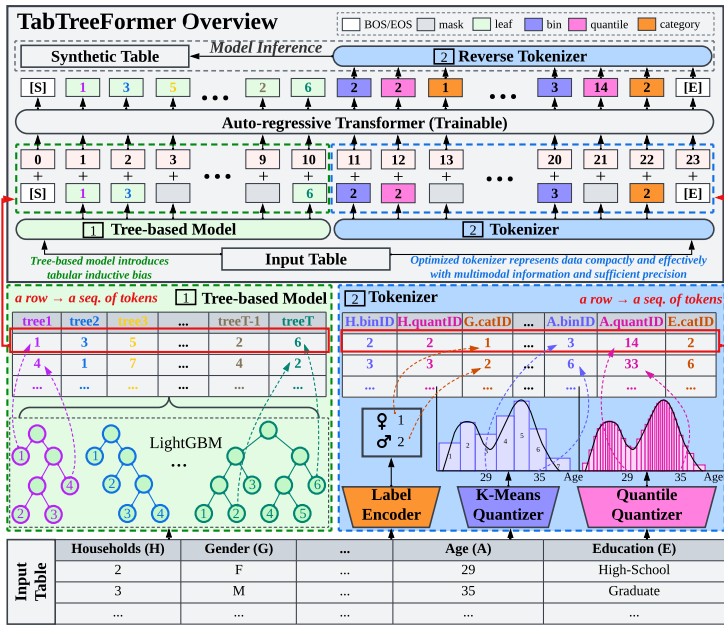


Figure 2: Overview of TabTreeFormer (data flow: bottom → top). It consists of 3 components: i) **a tree-based model** that introduces tabular-specific inductive biases; ii) **a tokenizer** that efficiently and compactly represents data while capturing multimodal distributions; iii) **a transformer model** that learns the priors extracted from the tree and tokenizer to generate high-quality synthetic data.

Table 1: Illustration of tokens in TabTreeFormer. “Size” indicates the number of tokens of this type. Recall Fig. 2 for the their colors and usage. “N” in “Format” can be any index in the range; e.g., leaf 3 ($3 < n_l$) is represented as [leaf3], corresponding to the light green tokens in Fig. 2 with value 3.

Type (Alias)	Size	Format	Source	Description
Leaf	$n_l = \max_{i \in \{1, 2, \dots, T\}} l_i$	[leafN]	Tree-based model \mathcal{T}	Leaf index in a tree
Categorical (cat)	$n_c = \max_{i \in \{1, 2, \dots, n\}} c_i$	[catN]	Data tokenizer \mathcal{D} (categorical columns)	Category ID
Cluster (bin)	$n_b = \max_{i \in \{1, 2, \dots, n\}} b_i$	[binN]	Data tokenizer \mathcal{D} (numeric columns)	Bin ID in K-Means quantizer
Quantile (quant)	$n_q = \max_{i \in \{1, 2, \dots, n\}} q_i$	[quantN]	Data tokenizer \mathcal{D} (numeric columns)	Quant. ID in quant. quantizer
Special	3	[BOS] [EOS] [mask]	Classical special tokens for LMs	BOS, EOS, and mask tokens

3.1 Tree-based Model

To inject tabular-specific inductive biases, we incorporate a tree-based model into the transformer (“Tree-based Model” in Fig. 2) by augmenting each row’s token sequence with leaf indices from a fitted tree model \mathcal{T} with T trees. Let $l_k \in \mathbb{N}$ be the number of leaves in k -th tree, where $k \in \{1, \dots, T\}$. In tree \mathcal{T} , the leaf index matrix $\mathbf{J} = [j_{ik}] \in \mathbb{N}^{n \times T}$ captures the position of each row \mathbf{X}_i in each tree. These indices encode non-smooth and non-rotationally invariant structure, enabling the model to possess these inductive biases of tabular data. By prepending leaf indices to input tokens, we transfer tree-based inductive biases to the transformer. During inference, these indices also act as prompts and guide towards more realistic data generation.

Many early tabular generation frameworks use conditional generation [64, 67], which improves the generation quality noticeably. These conditions are based on the values of a specific column in the dataset. In TabTreeFormer, we extend the condition of generation to clusters of the data and allow multiple concurrent conditions in place. Conceptually, each tree of a well-trained tree-based model provides an informative clustering of the training set, and the leaf index matrix provides a number of such clusterings. Therefore, providing the leaf indices as prompts, serving as conditions for generation, where multiple concurrent conditions (clusters) are provided and each condition features the clustering on one tree, is expected to be an effective generation performance booster.

3.2 Tokenizer

To model multimodal distributions and reduce both vocabulary size and sequence length, we design a tailored dual-quantization tokenizer for tabular data (“Tokenizer” in Fig. 2). For each continuous feature, we quantize the values so that it is of a more natural data format for transformers to learn. However, unlike TabMT [22] that uses a single quantizer, we use a dual-quantizer (i.e., double quantizers) to capture multimodal continuous distribution and describe the precise values respectively. Transformers do not expect near-Gaussian-distributed input tokens, so we capture the multimodal distribution simply by a K-Means quantizer [35] with a small number of clusters (e.g., $K = 10$). Following that, the original value is then quantized into a large number of quantiles (e.g., $Q = 1000$), based on which original values are recovered, and thus the values are highly precise. Employing the dual-quantization tokenization scheme, each numeric value is encoded into two discrete values: a bin ID in the K-Means quantizer and a quantile ID in the quantile quantizer, allowing two tokens to represent a numeric value with valuable and sufficient information. Categorical features are simply tokenized by label encoding, requiring 1 token. Formally, a reversible data tokenizer \mathcal{D} can be fitted on \mathbf{X} . Let $c_i \in \mathbb{N}$, $b_i \in \{0, \dots, K\}$, $q_i \in \{0, \dots, Q\}$ denote the number of categories, K-Means bins, and quantiles in i -th column respectively, where $c_i = 0$ in continuous features and $b_i = q_i = 0$ in categorical features. Then, the domain for a categorical value is $\{1, \dots, c_i\} \subseteq \mathbb{N}^+$, and the domain for a continuous value is $\{1, \dots, b_i\} \times \{1, \dots, q_i\} \subseteq (\mathbb{N}^+)^2$. A summary is seen in Table 1.

3.3 Transformer

TabTreeFormer is simply trained as an auto-regressive transformer. The input token sequence is constructed by concatenating the outcome from the tree model and tokenizer. It requires 5 types of tokens and a vocabulary size of $V = n_l + n_c + n_b + n_q + 3$. The number of tokens in a sequence corresponding to one row is $L = 2 + T + m_d + 2m_c$, including BOS and EOS tokens. Both the vocabulary size and sequence length are much smaller than the need for natural language models. A shared set of leaf tokens across all trees and similarly shared sets of category, bin, and quantile tokens across all features are used. Distinctions between different trees and features are effectively encoded through positional information, leveraging the positional embeddings inherent in most transformers.

A key observation on the construction of token sequence is that the valid range of tokens at each position is fixed for a given table. Consequently, tokens can be sampled exclusively from this precomputed set of valid options during generation. This ensures that every generated token sequence corresponds to a valid row, eliminating the need for rejecting invalid sequences [5, 55, 68], thus significantly accelerating the sampling process.

Additionally, transformers are prone to memorization, particularly when trained on tabular data, where datasets are much smaller compared to typical natural language corpora [5]. To avoid memorization, we heavily mask the input and maintain the target output unmasked. Moreover, we evenly split the training set into 2 subsets, one neural network (i.e., transformer in TabTreeFormer) is trained on one subset and validated on the other. Consequently, the validation loss can be a criterion for early stopping to avoid overfitting, too. When generating samples, we sample from the two networks with equal probability.

Theorem 1. *Given a real dataset \mathbf{X} , train M generative models $(\mathcal{G}_1, \mathcal{G}_2, \dots, \mathcal{G}_M)$ on an M -partition of it ($\mathbf{X} = [\mathbf{X}^{[1]}; \mathbf{X}^{[2]}; \dots; \mathbf{X}^{[M]}]$). If the generators are well-trained (distribution p of the corresponding partition is learned), then to sample \mathbf{X}' , sample data from \mathcal{G}_i for a probability of $|\mathbf{X}^{[i]}| / |\mathbf{X}|$ where $|\cdot|$ means the number of rows, we will have the resulting $p(\mathbf{X}') = p(\mathbf{X})$.*

Theorem 1 validates a generalized case of the method with two evenly split subsets described above, and can be trivially proven by the chain rule, so the proof is omitted. The rest of the training and generation settings are similar to the training and generation of classical causal language models, except for a modified embedding and loss function to account for the ordinal relations between quantile tokens, with details introduced in Section 3.4.

3.4 Embedding and Loss Function for Ordinal Tokens

Quantile Embeddings (QE) with Ordinal Relations. The known ordinal relation between quantile tokens resembles the known relative sequential relation between positions. Therefore, analogous to function-generated positional embeddings [58], we use function-generated embeddings for quantile tokens. Unlike positional tokens, which emphasize relative values, quantile tokens focus on absolute values, so we replace periodic trigonometric functions with non-linear monotonic scaled sigmoid functions for embedding generation. The embedding value generators are provided in Equation 3, where $i \in \{0, \dots, Q-1\}$ stands for the quantile ID, and $d \in \{0, \dots, D-1\}$ stands for the embedding dimensions. More detailed intuition and description of the function are provided in Appendix B.

$$S_d = \left\lfloor \frac{1 + \sqrt{1 + 4d}}{2} \right\rfloor \in \mathbb{N}^+ \quad (\text{scale factor}) \quad O_d = \frac{-4S_d^3 + (4d + 2)S_d}{2S_d - 1} \in [-2S_d, 2S_d] \quad (\text{offset}) \quad (2)$$

$$QE_{id} = \text{sigmoid} \left(4S_d \left(\frac{i}{Q} - \frac{1}{2} \right) + O_d \right) \quad (3)$$

Theorem 2. *Following the quantile embedding values in Equation 3, and let the embedded vector of quantile i be $\mathbf{q}_i = (QE_{i0} \ \dots \ QE_{i(D-1)}) \in (0, 1)^D$. For any $p \geq 1$, given quantile IDs $i, j, k \in \{0, \dots, Q-1\}$, and j, k are on the same side of i (i.e., $(i-j)(i-k) \geq 0$), then $|i-j| < |i-k|$ if and only if $\|\mathbf{q}_i - \mathbf{q}_j\|_p < \|\mathbf{q}_i - \mathbf{q}_k\|_p$, where $\|\cdot\|_p$ stands for the p -norm of a vector.*

Theorem 2 shows that the trend of the distance between the embedded vectors is consistent with the difference between quantile IDs. The mathematical proof is provided in Appendix B.5. At different embedding dimensions, we apply different slopes (by scale factor) and intercepts (by offset) on the input to sigmoid. Note that while the meaning of positions in a transformer is fixed, the interpretation of quantiles can vary across datasets. As a result, instead of fixing the embedding values as in Equation 3, we initialize the values by the equations, and they are updated during training. Non-quantile tokens will use a typical word token embedding layer of transformers.

Ordinal Cross-Entropy Loss. Cross-entropy loss (CEL) is typically used as the optimization objective of transformers. However, the quantized quantile tokens retain an inherent ordinal property, where closer IDs correspond to closer values. This relationship is not captured by standard CEL, where all classes are equally distinct. To address this, we replace the vanilla CEL with a specialized ordinal CEL for quantile tokens. Formally, let the predicted logits for a token be $\mathbf{z} \in \mathbb{R}^V$, the probability after softmax be $\mathbf{p} \in [0, 1]^V$ ($\|\mathbf{p}\|_1 = 1$), and the target label be $t \in \{1, \dots, V\}$. We

define *ordinal cross-entropy loss* (OCEL) as a weighted version of CEL. These weights are applied to unnormalized probabilities in both the numerator and denominator, depending on the current- and target-class pairs. It contrasts with the classical weighted CEL, which weights the loss per class based solely on the target class and applies to the numerator only. Formally, we write it as Equation 5 (recall the classical CEL in Equation 4), where w_{ti} denotes the weight for z_i , where t is the target class.

$$\mathcal{L}_{ce}(\mathbf{z}, t) = -\log \frac{e^{z_t}}{\sum_{i=1}^V e^{z_i}} = -\log p_t \quad (4) \quad \mathcal{L}_{oce}(\mathbf{z}, t) = -\log \frac{w_{tt} e^{z_t}}{\sum_{i=1}^V w_{ti} e^{z_i}} \quad (5)$$

Lemma 1. *Given $\mathbf{w} > \mathbf{0}$ independent of \mathbf{z} , OCEL is optimized when $z_t \rightarrow \infty$ and $z_i \rightarrow -\infty, \forall i \neq t$.*

Theorem 3. *Let $f(|t - i|)$ be a variant of the distance between current class i and target class t when f is non-negative and monotonically increasing. Let the weighted sum of this variant of distances to target incurred by some logit \mathbf{z} be $D(\mathbf{z}) = \sum_{i=1}^V p_i w_i$. If $w_{ti} = f(|t - i|)$ for some f , then for \mathbf{z}, \mathbf{z}^* with $\mathcal{L}_{ce}(\mathbf{z}, t) = \mathcal{L}_{ce}(\mathbf{z}^*, t)$ and $D(\mathbf{z}) < D(\mathbf{z}^*)$, we must have $\mathcal{L}_{oce}(\mathbf{z}, t) < \mathcal{L}_{oce}(\mathbf{z}^*, t)$.*

Both Lemma 1 and Theorem 3 are intuitive, and we provide rigorous proofs in Appendix C.1-C.2. Theorem 3 implies that the OCEL penalizes (value being smaller) classes closer to the target class less than farther ones. Any definition of $w_{ti} = f(|t - i|)$ satisfying the monotonicity constraint works for OCEL technically. In this paper, we define the weight w_{ti} for z_i to be obtained by Equation 6.

$$w_{ti} = 1 + m - e^{-\frac{(t-i)^2}{(V\sigma)^2}} \quad (6)$$

where $\sigma = 0.005$ is a scaling factor of the distance, and $m = 0.5$ is the minimum weight (used on $i = t$). Detailed explanation and analysis of it can be found in Appendix C.3.

Note that not all tokens are part of the ordinal relation, so the OCEL is applied only to valid quantile tokens at the corresponding positions. To enable the model to learn to generate valid quantile tokens, we introduce an additional modified CEL to distinguish valid tokens from invalid ones, which complements OCEL. See Appendix C.4 for the exact overall loss formula.

4 Experiments

4.1 Experimental Setup

Basic Setup. For all datasets, we split train and test sets in 4 : 1, and repeat each experiment 3 times and report the results. We conduct all experiments on a machine equipped with 1 NVIDIA RTX 4090 and 20 CPU cores. Detailed environment setting can be found in Appendix D.1.

TabTreeFormer Implementation. We use LightGBM [31] whose hyperparameters are tuned by Optuna [1] as the tree-based model. We exploit Distill-GPT2 [50] as the transformer backbone, following the practice in prior works [5, 55]. TabTreeFormer (TTF) is experimented with two major configurations: S (small) and L (large), with the number of trainable parameters of approximately 5M and 40M, respectively. When privacy and efficiency are not crucial concerns, we remove the masks and make other changes accordingly to TTF-L, which we call TTF-NM (**no mask**). In ablation study, we use TabTreeFormer-S. Implementation and setting details can be found in Appendix A.

Datasets. Experiments are conducted on 9 datasets with diverse sizes and characteristics from OpenML [57]: adult, bank, boston, breast, credit, diabetes, iris, qsar, and wdbc. When doing ablation study, we use credit and diabetes. Details of these datasets are summarized in Appendix D.2.

Baseline Models. We compare the performance of TabTreeFormer against 8 SOTA methods in tabular data generation, including non-neural networks, GANs, VAEs, diffusion models, and autoregressive transformers (ART) or masked transformers: Forest Diffusion (FD) [30], CTAB-GAN+ (CTAB+) [69], TTVAE [59], TabSyn [65], GReaT [5], REaLTabFormer (RTF) [55], TabMT [22], and TabuLa [68]. Justification of the baseline choices and implementation details are described in Appendix D.3.

Metrics. We comprehensively evaluate TabTreeFormer using utility, fidelity, privacy, and efficiency, which are standard metrics in tabular data generation [64, 69, 5, 65, 51]. Detailed implementation of the metrics can be found in Appendix D.4-D.6.

Table 2: Averaged MLE performance of different models on all 9 datasets. RE stands for relative error (w.r.t. score on real data). Avg. stands for the average raw MLE score. The best scores and the second best scores are highlighted in bold with and without underscore, respectively.

ML	Real	FD [30]	CTAB+ [69]	TTVAE [59]	TabSyn [65]	GReaT [5]	RTF [55]	TabMT [22]	TabuLa ¹ [68]	TTF-S	TTF-L	TTF-NM
RE ² (↓)	all		0.020 _{±0.033}	0.253 _{±0.287}	0.203 _{±0.335}	0.024 _{±0.030}	0.117 _{±0.178}	0.027 _{±0.042}	0.062 _{±0.103}	0.041 _{±0.051}	0.031 _{±0.040}	0.021 _{±0.035}
	LN		0.014 _{±0.027}	0.231 _{±0.260}	0.249 _{±0.476}	0.025 _{±0.036}	0.095 _{±0.131}	0.023 _{±0.033}	0.056 _{±0.089}	0.037 _{±0.066}	0.025 _{±0.035}	0.019 _{±0.032}
	RF		0.020 _{±0.027}	0.256 _{±0.293}	0.184 _{±0.275}	0.019 _{±0.024}	0.127 _{±0.202}	0.025 _{±0.037}	0.064 _{±0.107}	0.045 _{±0.049}	0.031 _{±0.037}	0.018 _{±0.045}
	XGB		0.026 _{±0.044}	0.272 _{±0.337}	0.175 _{±0.242}	0.028 _{±0.031}	0.130 _{±0.210}	0.034 _{±0.056}	0.067 _{±0.116}	0.041 _{±0.046}	0.036 _{±0.050}	0.026 _{±0.032}
Avg. (↑)	all	0.899 _{±0.104}	0.884 _{±0.122}	0.685 _{±0.285}	0.747 _{±0.312}	0.880 _{±0.119}	0.807 _{±0.215}	0.878 _{±0.129}	0.853 _{±0.168}	0.840 _{±0.129}	0.875 _{±0.126}	0.881 _{±0.113}
	LN	0.891 _{±0.125}	0.881 _{±0.144}	0.695 _{±0.272}	0.719 _{±0.405}	0.872 _{±0.145}	0.818 _{±0.200}	0.874 _{±0.143}	0.851 _{±0.182}	0.835 _{±0.160}	0.872 _{±0.141}	0.875 _{±0.135}
	RF	0.901 _{±0.104}	0.885 _{±0.119}	0.686 _{±0.289}	0.757 _{±0.286}	0.884 _{±0.109}	0.801 _{±0.233}	0.881 _{±0.127}	0.852 _{±0.171}	0.839 _{±0.124}	0.875 _{±0.125}	0.883 _{±0.105}
	XGB	0.906 _{±0.094}	0.886 _{±0.122}	0.673 _{±0.326}	0.765 _{±0.262}	0.883 _{±0.113}	0.803 _{±0.236}	0.880 _{±0.131}	0.854 _{±0.171}	0.848 _{±0.116}	0.878 _{±0.127}	0.885 _{±0.112}
<hr/>												
Table 3: Averaged fidelity performance of different models on all 9 datasets. The best scores and the second best scores are highlighted in bold with and without underscore, respectively.												
FD [30]	CTAB+ [69]	TTVAE [59]	TabSyn [65]	GReaT [5]	RTF [55]	TabMT [22]	TabuLa [68]	TTF-S	TTF-L	TTF-NM		
Shape 0.931 _{±0.047}	0.890 _{±0.067}	0.736 _{±0.150}	0.925 _{±0.052}	0.881 _{±0.062}	0.924 _{±0.067}	0.919 _{±0.052}	0.916 _{±0.076}	0.910 _{±0.037}	0.915 _{±0.042}	0.894 _{±0.081}		
Trend 0.922 _{±0.064}	0.813 _{±0.122}	0.678 _{±0.219}	0.911 _{±0.084}	0.862 _{±0.088}	0.899 _{±0.091}	0.912 _{±0.065}	0.894 _{±0.085}	0.901 _{±0.069}	0.913 _{±0.076}	0.908 _{±0.098}		

- **Utility** exhibits the quality of synthetic data by testing its performance on downstream tasks. We evaluate based on the established Train-on-Synthetic, Test-on-Real (TSTR) machine learning efficacy (MLE) evaluation framework [64], namely, synthetic data generated based on real training data is tested on a hold-out real test set. Three models are used: linear (i.e., linear and logistic regression; LN), random forest (RF) [7], and XGBoost (XGB) [10]. Classification performance is evaluated by weighted AUC ROC and regression is evaluated by R^2 . For both metrics, better generative models tend to yield higher scores on downstream tasks. MLE is the most widely used synthetic tabular data generation evaluation metric, which is reported in all baselines, while no other metrics have a comparable prevalence, so we treat this as the core synthetic data quality score.
- **Fidelity** shows the cosmetic discrepancy between the real and synthetic data. It is evaluated via “Shape” and “Trend” metrics [13, 51]. “Shape” measures the similarity of marginal distribution density for each column, and “Trend” measures the fidelity in correlation between column pairs. Higher “Shape” and “Trend” values indicate better data fidelity.
- **Privacy** is a crucial criterion when the synthetic data serves the use case of privacy-preserving data sharing. We use the distance to the closest record (DCR) [67] to evaluate the privacy of synthetic data. We compare the DCR from synthetically generated data and from hold-out real (test) data to the real training data and privacy preservation is demonstrated by DCRs calculated on the latter being no smaller than the former, tested by Mann-Whitney U Test [36]. Privacy is at risk of disclosure when p -values are smaller than 0.05.
- **Efficiency** showcases the model sizes and computation time for training and generation of different models. Under comparable performance, smaller models and faster computation are favored.

4.2 Synthetic Data Quality (Utility and Fidelity)

Table 2-3 shows a summary of synthetic quality metric scores, on utility and fidelity respectively. Raw scores on individual datasets are found in Table 10-Table 11 in Appendix E.1.

Utility: MLE. The MLE results show that TabTreeFormer-NM outperforms baseline models across different dataset and ML model used in general. Recall that MLE is considered the core quality metric, so the MLE result demonstrates our model’s outstanding capability in generating high-quality synthetic data. Moreover, TabTreeFormer’s advantage over baselines is more obvious on better downstream models (assume XGB>RF>LN), which indicates TabTreeFormer’s ability in capturing implicit and complex relations, manifested by the introduction of tree-based model.

Fidelity: Marginal density distribution of columns (Shape). TabTreeFormer achieves comparable performance to baseline models in “Shape” metric, especially to ART-based baseline models. Meanwhile, Fig. 3 shows that TabTreeFormer captures better multimodal distribution compared to other ARTs, which validates the effectiveness of our dual-quantization tokenizer design.

¹For TabuLa, 2/9 datasets fail to generate reasonable data under the default setting.

²The reported utility improvement in abstract and introduction is computed from this row.

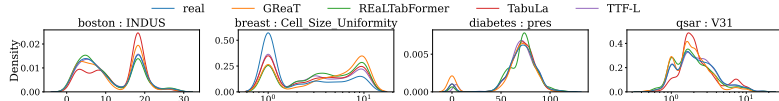


Figure 3: Marginal densities of representative multimodal continuous columns from baseline ART and TTF. All have a Distill-GPT2 backbone.

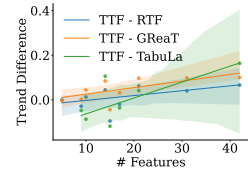


Figure 5: Feature count vs. Trend score improvement of TTF from ART baselines.

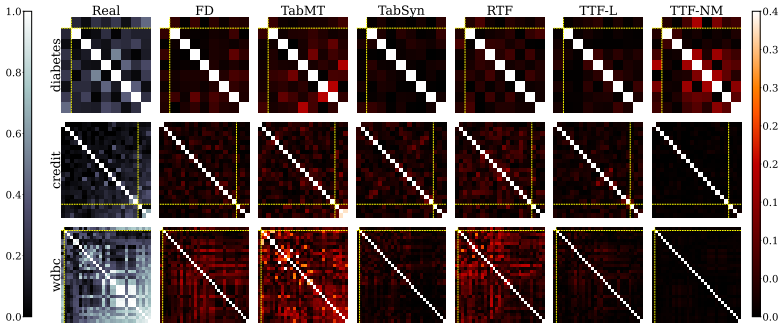


Figure 4: TTF versus top-4 baselines in pair-wise correlation. Real (absolute) correlation values are presented on the left, and the absolute error in correlation values in synthetic data from different models, capped at 0.4 for visibility, are shown at the right (the darker the better). The left-top features (divided by yellow line) are categorical and the right-bottom are numeric.

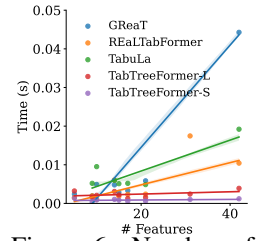


Figure 6: Number of features vs. average generation time per (valid) row of TTF and ART baselines.

Fidelity: Pair-wise correlation between columns (Trend). TabTreeFormer-L outperforms all neural network baselines in “Trend”, implying the superior capability of TabTreeFormer in learning inter-feature relations. We also visualize the pair-wise correlation of some datasets in Fig. 4. While TabTreeFormer-NM is able to capture the correlations on some datasets perfectly, its performance variance across datasets is large. In addition, TabTreeFormer tends to show a more significant improvement from ART baselines with more features, as referred in Fig. 5. This demonstrates the advantage of introducing the inductive bias to address low-correlations so that models learn better by filtering out less correlated features, which is more common with more features.

4.3 Balancing Synthetic Data Quality with Privacy and Efficiency

Privacy: DCR. As summarized in Table 4, TabTreeFormer-S and L are privacy-resilient in all the 9 datasets. In comparison, Forest Diffusion [30] has privacy issues in 5 out of 9 datasets, which is consistent with our analysis in Section 2.2 on its potential privacy issues. As for ART baseline methods, all but GReaT [5] demonstrates privacy risk to some extent, particularly TabuLa [68], which bears severe privacy leakage concerns in 5 out of 7 successfully run datasets. This result also verifies that the masking and early stopping of TabTreeFormer’s design successfully protects privacy. Raw p -values per experiment are presented in Table 12 in Appendix E.2.

Efficiency: Model Parameters. The efficiency of TabTreeFormer is mainly demonstrated by its ability to achieve comparable performance with a significantly smaller model size. Although TabTreeFormer-L is better than TabTreeFormer-S in general, demonstrating the usefulness of a larger model, TabTreeFormer-S achieves comparable utility with the best-performing ART baseline (RReaLTabFormer [55], which has only marginally better MLE results than TabTreeFormer-S), while the baseline models have more than 80M parameters.

Table 4: Privacy performances. The first two rows are the average and minimum p -values, and the last row shows the number of violations (i.e., $p < 0.05$). The closer the p -value to 0, the higher the risk of privacy leakage. Non-zero violations are highlighted in red, indicating privacy risks.

	FD	CTAB+ TTVAE	TabSyn	GReaT	RTF	TabMT	TabuLa	TTF-S	TTF-L	TTF-NM
Avg. p	0.380	1.000	0.904	0.559	0.843	0.394	0.865	0.251	0.933	0.745
Min. p	0.000	1.000	0.382	0.029	0.082	0.000	0.259	0.000	0.662	0.214
# vio.	5	0	1	0	3	0	5	0	0	3

Table 5: Average computation time (s) of TabTreeFormer and other ART baselines. The best values are highlighted in bold with an underscore, and the second best values are highlighted in bold without underscore.

	GReaT [5]	RTF [55]	TabuLa [68]	TTF-S	TTF-L
Train	2470.344	359.950	718.260	316.743	773.362
Generate	45.998	24.932	74.702	7.846	19.718

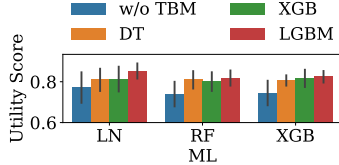


Figure 7: Utility of different tree-based model in TTF. The x -axis shows the downstream model type.

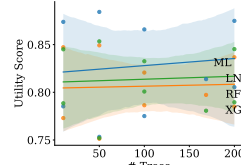


Figure 8: Utility of different number of trees in the tree-based model in TTF.

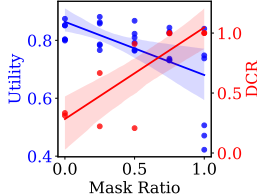


Figure 9: Quality & privacy trend of different mask ratios.

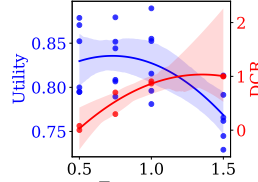


Figure 10: Quality & privacy trend of different temperatures.

Table 6: Design component ablation. Average utility scores are reported. All experiments are based on variants of TabTreeFormer-S.

ML	all	LN	RF	XGB
TTF-S	0.832	0.853	0.818	0.824
gen. w/o tree	0.792	0.808	0.780	0.789
w/o OCEL	0.809	0.825	0.802	0.800
w/o QE	0.801	0.820	0.783	0.799

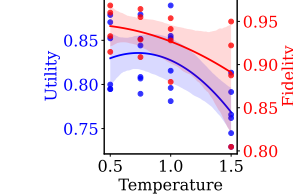


Figure 11: Utility & fidelity trend of different temperatures.

Efficiency: Computation Time. Comparing TabTreeFormer with all other ART baselines in terms of computation time, as shown in Table 5, TabTreeFormer demonstrates a steady advantage in terms of generation time. This advantage is particularly obvious on datasets with a larger number of features, as shown in Fig. 6, showing the effect on generation efficiency of using a standard and aligned sequence format and sampling tokens by filtering out invalid tokens according to the format. Raw training and generation time records can be found in Table 14 in Appendix E.3.

4.4 Ablation Study

Effect of Tree-based Models. A core design of TabTreeFormer is its integration of a tree-based model. As shown in Fig. 7, having a tree-based model integrated is helpful. However, the exact tree-based model used does not seem to make a significant difference, though a subtle trend that multiple-tree models (XGBoost [10] and LightGBM [31]) are better than single-tree model (decision tree (DT) [6]) can be observed. Nevertheless, observing the effect of the number of trees on multiple-tree models, as shown in Fig. 8, no obvious trend can be observed either, though there is still a general but very subtle trend that more trees result in better performance.

TabTreeFormer-NM Settings. Two core settings of NM different from L version is the mask ratio and temperature, so we also look at how the two parameters affect the performance, as shown in Fig. 9-11. The utility and DCR changes with mask ratio and demonstrate demonstrates clearly the dilemma between synthetic data quality and privacy, and as expected, the larger ratio is masked or the larger temperature, the better privacy and worse utility. Nevertheless, Fig. 11 shows a slight different trend on performance of utility and fidelity on temperature. As we maximize the synthetic data quality mainly by utility, it is likely that the temperatures is not maximized with the fidelity, which explains the reason for TabTreeFormer’s score in fidelity (recall Table 3) not being the best.

Other Core Design Components. We also validate the effectiveness of other important design components: generation with tree-leaf tokens as prompts (vs. gen. w/o tree), training with OCEL (vs. w/o OCEL), and training with quantile embedding implementation (vs. w/o QE). The result is shown in Table 6. All the three components have a significant impact on improving the performance.

5 Conclusion

In this paper, we propose TabTreeFormer, a hybrid tree-transformer based model for high-quality tabular data generation. It combines tree-based inductive biases with a dual-quantization tokenizer to model multimodal numeric distributions, and specialized loss and embeddings applied on quantized ordinal tokens. When evaluated on nine datasets against eight baselines, TabTreeFormer achieves stronger balance on quality, privacy, and efficiency, and particularly excels in data utility when privacy and efficiency are not prioritized.

Acknolwedgements

We would like to acknowledge Rishav Chourasia for helpful discussions.

References

- [1] Takuya Akiba, Shotaro Sano, Toshihiko Yanase, Takeru Ohta, and Masanori Koyama. Optuna: A next-generation hyperparameter optimization framework. In Ankur Teredesai, Vipin Kumar, Ying Li, Rómer Rosales, Evinaria Terzi, and George Karypis, editors, *Proceedings of the 25th ACM SIGKDD International Conference on Knowledge Discovery & Data Mining, KDD 2019, Anchorage, AK, USA, August 4-8, 2019*, pages 2623–2631. ACM, 2019. doi: 10.1145/3292500.3330701.
- [2] Sercan Ö. Arik and Tomas Pfister. TabNet: Attentive interpretable tabular learning. *Proceedings of the AAAI Conference on Artificial Intelligence*, 35(8):6679–6687, May 2021. doi: 10.1609/aaai.v35i8.16826.
- [3] Samuel A. Assefa, Danial Dervovic, Mahmoud Mahfouz, Robert E. Tillman, Prashant Reddy, and Manuela Veloso. Generating synthetic data in finance: opportunities, challenges and pitfalls. In *Proceedings of the First ACM International Conference on AI in Finance, ICAIF '20*, New York, NY, USA, 2021. Association for Computing Machinery. ISBN 9781450375849. doi: 10.1145/3383455.3422554.
- [4] Christopher M. Bishop. *Pattern Recognition and Machine Learning (Information Science and Statistics)*. Springer-Verlag, Berlin, Heidelberg, 2006. ISBN 0387310738.
- [5] Vadim Borisov, Kathrin Seßler, Tobias Leemann, Martin Pawelczyk, and Gjergji Kasneci. Language models are realistic tabular data generators. In *The Eleventh International Conference on Learning Representations, ICLR 2023, Kigali, Rwanda, May 1-5, 2023*. OpenReview.net, 2023.
- [6] L. Breiman, Jerome H. Friedman, Richard A. Olshen, and C. J. Stone. Classification and regression trees. *Biometrics*, 40:874, 1984. URL <https://api.semanticscholar.org/CorpusID:29458883>.
- [7] Leo Breiman. Random forests. *Machine learning*, 45(1):5–32, 2001. ISSN 1573-0565. doi: 10.1023/A:1010933404324.
- [8] Wenzhi Cao, Vahid Mirjalili, and Sebastian Raschka. Rank consistent ordinal regression for neural networks with application to age estimation. *Pattern Recognition Letters*, 140:325–331, 2020. ISSN 0167-8655. doi: <https://doi.org/10.1016/j.patrec.2020.11.008>.
- [9] François Castagnos, Martin Mihelich, and Charles Dognin. A simple log-based loss function for ordinal text classification. In Nicoletta Calzolari, Chu-Ren Huang, Hansaem Kim, James Pustejovsky, Leo Wanner, Key-Sun Choi, Pum-Mo Ryu, Hsin-Hsi Chen, Lucia Donatelli, Heng Ji, Sadao Kurohashi, Patrizia Paggio, Nianwen Xue, Seokhwan Kim, Youngyun Hahm, Zhong He, Tony Kyungil Lee, Enrico Santus, Francis Bond, and Seung-Hoon Na, editors, *Proceedings of the 29th International Conference on Computational Linguistics*, pages 4604–4609, Gyeongju, Republic of Korea, October 2022. International Committee on Computational Linguistics.
- [10] Tianqi Chen and Carlos Guestrin. XGBoost: A scalable tree boosting system. In Balaji Krishnapuram, Mohak Shah, Alexander J. Smola, Charu C. Aggarwal, Dou Shen, and Rajeev Rastogi, editors, *Proceedings of the 22nd ACM SIGKDD International Conference on Knowledge Discovery and Data Mining, San Francisco, CA, USA, August 13-17, 2016*, pages 785–794. ACM, 2016. doi: 10.1145/2939672.2939785.
- [11] Zihang Dai, Zhilin Yang, Yiming Yang, Jaime G. Carbonell, Quoc Viet Le, and Ruslan Salakhutdinov. Transformer-xl: Attentive language models beyond a fixed-length context. In Anna Korhonen, David R. Traum, and Lluís Màrquez, editors, *Proceedings of the 57th Conference of the Association for Computational Linguistics, ACL 2019, Florence, Italy, July 28- August 2, 2019, Volume 1: Long Papers*, pages 2978–2988. Association for Computational Linguistics, 2019. doi: 10.18653/V1/P19-1285.
- [12] Sabyasachi Dash, Sushil Kumar Shakyawar, Mohit Sharma, and Sandeep Kaushik. Big data in healthcare: management, analysis and future prospects. *Journal of Big Data*, 6(1):54, 2019. ISSN 2196-1115. doi: 10.1186/s40537-019-0217-0.
- [13] *Synthetic Data Metrics*. DataCebo, Inc., 12 2023. URL <https://docs.sdv.dev/sdmetrics/>. Version 0.13.0.
- [14] Raul Diaz and Amit Marathe. Soft labels for ordinal regression. In *Proceedings of the IEEE/CVF Conference on Computer Vision and Pattern Recognition (CVPR)*, June 2019.
- [15] Alexey Dosovitskiy, Lucas Beyer, Alexander Kolesnikov, Dirk Weissenborn, Xiaohua Zhai, Thomas Unterthiner, Mostafa Dehghani, Matthias Minderer, Georg Heigold, Sylvain Gelly, Jakob Uszkoreit, and Neil Houlsby. An image is worth 16x16 words: Transformers for image recognition at scale. In *9th International Conference on Learning Representations, ICLR 2021, Virtual Event, Austria, May 3-7, 2021*. OpenReview.net, 2021.

[16] EU. Regulation (EU) 2016/679 of the European parliament and of the council of 27 April 2016 on the protection of natural persons with regard to the processing of personal data and on the free movement of such data, and repealing directive 95/46/EC (General Data Protection Regulation). *OJ*, L 119, Apr 2016. URL <https://gdpr-info.eu/>.

[17] R. A. Fisher. The use of multiple measurements in taxonomic problems. *Annals of Eugenics*, 7(2):179–188, Sep 1936. doi: 10.1111/j.1469-1809.1936.tb02137.x.

[18] Ian Goodfellow, Jean Pouget-Abadie, Mehdi Mirza, Bing Xu, David Warde-Farley, Sherjil Ozair, Aaron Courville, and Yoshua Bengio. Generative adversarial nets. In Z. Ghahramani, M. Welling, C. Cortes, N. Lawrence, and K.Q. Weinberger, editors, *Advances in Neural Information Processing Systems*, volume 27. Curran Associates, Inc., 2014.

[19] Yury Gorishniy, Ivan Rubachev, Valentin Khrulkov, and Artem Babenko. Revisiting deep learning models for tabular data. In M. Ranzato, A. Beygelzimer, Y. Dauphin, P.S. Liang, and J. Wortman Vaughan, editors, *Advances in Neural Information Processing Systems*, volume 34, pages 18932–18943, Red Hook, NY, USA, 2021. Curran Associates, Inc. ISBN 9781713845393.

[20] Yury Gorishniy, Ivan Rubachev, and Artem Babenko. On embeddings for numerical features in tabular deep learning. In S. Koyejo, S. Mohamed, A. Agarwal, D. Belgrave, K. Cho, and A. Oh, editors, *Advances in Neural Information Processing Systems*, volume 35, pages 24991–25004. Curran Associates, Inc., 2022.

[21] Léo Grinsztajn, Edouard Oyallon, and Gaël Varoquaux. Why do tree-based models still outperform deep learning on typical tabular data? In S. Koyejo, S. Mohamed, A. Agarwal, D. Belgrave, K. Cho, and A. Oh, editors, *Advances in Neural Information Processing Systems*, volume 35, pages 507–520, Red Hook, NY, USA, 2022. Curran Associates, Inc. ISBN 9781713871088.

[22] Manbir Gulati and Paul Roysdon. TabMT: Generating tabular data with masked transformers. In A. Oh, T. Naumann, A. Globerson, K. Saenko, M. Hardt, and S. Levine, editors, *Advances in Neural Information Processing Systems*, volume 36, pages 46245–46254, Red Hook, NY, USA, 2023. Curran Associates, Inc.

[23] David Harrison and Daniel L Rubinfeld. Hedonic housing prices and the demand for clean air. *JEEM*, 5(1):81–102, 1978. ISSN 0095-0696.

[24] Mikel Hernandez, Gorka Epelde, Ane Alberdi, Rodrigo Cilla, and Debbie Rankin. Synthetic data generation for tabular health records: A systematic review. *Neurocomputing*, 493:28–45, 2022. ISSN 0925-2312. doi: <https://doi.org/10.1016/j.neucom.2022.04.053>.

[25] Jonathan Ho, Ajay Jain, and Pieter Abbeel. Denoising diffusion probabilistic models. In H. Larochelle, M. Ranzato, R. Hadsell, M.F. Balcan, and H. Lin, editors, *Advances in Neural Information Processing Systems*, volume 33, pages 6840–6851. Curran Associates, Inc., 2020.

[26] Hans Hofmann. Statlog (German Credit Data). UCI Machine Learning Repository, 1994. DOI: <https://doi.org/10.24432/C5NC77>.

[27] Noah Hollmann, Samuel Müller, Katharina Eggensperger, and Frank Hutter. TabPFN: A transformer that solves small tabular classification problems in a second. In *The Eleventh International Conference on Learning Representations, ICLR 2023, Kigali, Rwanda, May 1-5, 2023*. OpenReview.net, 2023.

[28] Le Hou, Chen-Ping Yu, and Dimitris Samaras. Squared earth mover’s distance-based loss for training deep neural networks. *CoRR*, abs/1611.05916, 2016. URL <http://arxiv.org/abs/1611.05916>.

[29] Xin Huang, Ashish Khetan, Milan Cvitkovic, and Zohar S. Karnin. TabTransformer: Tabular data modeling using contextual embeddings. *CoRR*, abs/2012.06678, 2020. URL <https://arxiv.org/abs/2012.06678>.

[30] Alexia Jolicoeur-Martineau, Kilian Fatras, and Tal Kachman. Generating and imputing tabular data via diffusion and flow-based gradient-boosted trees. In Sanjoy Dasgupta, Stephan Mandt, and Yingzhen Li, editors, *Proceedings of The 27th International Conference on Artificial Intelligence and Statistics*, volume 238 of *Proceedings of Machine Learning Research*, pages 1288–1296. PMLR, 02–04 May 2024.

[31] Guolin Ke, Qi Meng, Thomas Finley, Taifeng Wang, Wei Chen, Weidong Ma, Qiwei Ye, and Tie-Yan Liu. LightGBM: A highly efficient gradient boosting decision tree. In I. Guyon, U. Von Luxburg, S. Bengio, H. Wallach, R. Fergus, S. Vishwanathan, and R. Garnett, editors, *Advances in Neural Information Processing Systems*, volume 30, Red Hook, NY, USA, 2017. Curran Associates, Inc. ISBN 9781510860964.

[32] Diederik P. Kingma and Max Welling. Auto-encoding variational bayes. In Yoshua Bengio and Yann LeCun, editors, *2nd International Conference on Learning Representations, ICLR 2014, Banff, AB, Canada, April 14-16, 2014, Conference Track Proceedings*, 2014.

[33] Ron Kohavi. Scaling up the accuracy of Naive-Bayes classifiers: a decision-tree hybrid. In *Proceedings of the Second International Conference on Knowledge Discovery and Data Mining*, KDD'96, page 202–207. AAAI Press, 1996.

[34] Wanhua Li, Xiaoke Huang, Jiwen Lu, Jianjiang Feng, and Jie Zhou. Learning probabilistic ordinal embeddings for uncertainty-aware regression. In *Proceedings of the IEEE/CVF Conference on Computer Vision and Pattern Recognition (CVPR)*, pages 13896–13905, June 2021.

[35] J. MacQueen. Some methods for classification and analysis of multivariate observations. In Lucien M. Le Cam and Jerzy Neyman, editors, *Proceedings of the Fifth Berkeley Symposium on Mathematical Statistics and Probability*, volume 1, pages 281–297. University of California Press, Berkeley, CA, 1967.

[36] H. B. Mann and D. R. Whitney. On a test of whether one of two random variables is stochastically larger than the other. *The Annals of Mathematical Statistics*, 18(1):50 – 60, 1947. doi: 10.1214/aoms/1177730491.

[37] Kamel Mansouri, Tine Ringsted, Davide Ballabio, Roberto Todeschini, and Viviana Consonni. Quantitative structure–activity relationship models for ready biodegradability of chemicals. *Journal of Chemical Information and Modeling*, 53(4):867–878, 2013. doi: 10.1021/ci4000213. PMID: 23469921.

[38] Calvin McCarter. Unmasking trees for tabular data. *CoRR*, abs/2407.05593, 2024. doi: 10.48550/ARXIV.2407.05593. URL <https://doi.org/10.48550/arXiv.2407.05593>.

[39] Sérgio Moro, Paulo Cortez, and Raul Laureano. Using data mining for bank direct marketing: An application of the CRISP-DM methodology. In *Proceedings of the European Simulation and Modelling Conference*, 10 2011.

[40] Inbar Nachmani, Bar Genossar, Coral Scharf, Roee Shraga, and Avigdor Gal. SLACE: A monotone and balance-sensitive loss function for ordinal regression. *Proceedings of the AAAI Conference on Artificial Intelligence*, 39(18):19598–19606, Apr. 2025. doi: 10.1609/aaai.v39i18.34158.

[41] Aditya Narvekar and Shubh Mehta. Cat2Vec with position encoding: A new approach for handling ordinal features using learned embeddings with positional encoding. *International Journal of Computer Applications*, 186(44):9–15, Oct 2024. ISSN 0975-8887. doi: 10.5120/ijca2024924052.

[42] Andrew Y. Ng. Feature selection, L1 vs. L2 regularization, and rotational invariance. In *Proceedings of the Twenty-First International Conference on Machine Learning*, ICML '04, page 78, New York, NY, USA, 2004. Association for Computing Machinery. ISBN 1581138385. doi: 10.1145/1015330.1015435.

[43] Zhenxing Niu, Mo Zhou, Le Wang, Xinbo Gao, and Gang Hua. Ordinal regression with multiple output CNN for age estimation. In *2016 IEEE Conference on Computer Vision and Pattern Recognition (CVPR)*, pages 4920–4928, 2016. doi: 10.1109/CVPR.2016.532.

[44] Noseong Park, Mahmoud Mohammadi, Kshitij Gorde, Sushil Jajodia, Hongkyu Park, and Youngmin Kim. Data synthesis based on generative adversarial networks. *Proc. VLDB Endow.*, 11(10):1071–1083, Jun 2018. ISSN 2150-8097. doi: 10.14778/3231751.3231757.

[45] PDPC. Proposed guide on synthetic data generation. *Personal Data Protection Commission*, July 2024. URL <https://www.pdpc.gov.sg/help-and-resources/2024/07/proposed-guide-on-synthetic-data-generation>. Accessed: 2024-12-26.

[46] Liudmila Prokhorenkova, Gleb Gusev, Aleksandr Vorobev, Anna Veronika Dorogush, and Andrey Gulin. CatBoost: unbiased boosting with categorical features. In S. Bengio, H. Wallach, H. Larochelle, K. Grauman, N. Cesa-Bianchi, and R. Garnett, editors, *Advances in Neural Information Processing Systems*, volume 31, page 6639–6649, Red Hook, NY, USA, 2018. Curran Associates, Inc.

[47] Zhaozhi Qian, Rob Davis, and Mihaela van der Schaar. Synthcity: a benchmark framework for diverse use cases of tabular synthetic data. In A. Oh, T. Naumann, A. Globerson, K. Saenko, M. Hardt, and S. Levine, editors, *Advances in Neural Information Processing Systems*, volume 36, pages 3173–3188, Red Hook, NY, USA, 2023. Curran Associates, Inc.

[48] Alec Radford, Jeffrey Wu, Rewon Child, David Luan, Dario Amodei, and Ilya Sutskever. Language models are unsupervised multitask learners. *OpenAI Blog*, 1(8), 2019. URL https://cdn.openai.com/better-language-models/language_models_are_unsupervised_multitask_learners.pdf.

[49] Nasim Rahaman, Aristide Baratin, Devansh Arpit, Felix Draxler, Min Lin, Fred A. Hamprecht, Yoshua Bengio, and Aaron C. Courville. On the spectral bias of neural networks. In Kamalika Chaudhuri and Ruslan Salakhutdinov, editors, *Proceedings of the 36th International Conference on Machine Learning*, volume 97 of *Proceedings of Machine Learning Research*, pages 5301–5310. PMLR, 09–15 Jun 2019.

[50] Victor Sanh, Lysandre Debut, Julien Chaumond, and Thomas Wolf. DistilBERT, a distilled version of BERT: smaller, faster, cheaper and lighter. In *NeurIPS EMC2 Workshop*, 2019.

[51] Juntong Shi, Minkai Xu, Harper Hua, Hengrui Zhang, Stefano Ermon, and Jure Leskovec. TabDiff: a mixed-type diffusion model for tabular data generation. In *The Thirteenth International Conference on Learning Representations*, 2025.

[52] Xintong Shi, Wenzhi Cao, and Sebastian Raschka. Deep neural networks for rank-consistent ordinal regression based on conditional probabilities. *Pattern Anal. Appl.*, 26(3):941–955, June 2023. ISSN 1433-7541. doi: 10.1007/s10044-023-01181-9.

[53] Ravid Shwartz-Ziv and Amitai Armon. Tabular data: Deep learning is not all you need. *Inf. Fusion*, 81(C):84–90, May 2022. ISSN 1566-2535. doi: 10.1016/j.inffus.2021.11.011.

[54] Jack Smith, J. Everhart, W. Dickson, W. Knowler, and Richard Johannes. Using the ADAP learning algorithm to forecast the onset of diabetes mellitus. *Proc. Annu. Symp. Comput. Appl. Med. Care*, 10, 11 1988.

[55] Aivin V. Solatorio and Olivier Dupriez. REaLTabFormer: Generating realistic relational and tabular data using transformers. *CoRR*, abs/2302.02041, 2023. doi: 10.48550/ARXIV.2302.02041. URL <https://doi.org/10.48550/arXiv.2302.02041>.

[56] W. Nick Street, W. H. Wolberg, and O. L. Mangasarian. Nuclear feature extraction for breast tumor diagnosis. In Raj S. Acharya and Dmitry B. Goldgof, editors, *Biomedical Image Processing and Biomedical Visualization*, volume 1905, pages 861 – 870. International Society for Optics and Photonics, SPIE, 1993.

[57] Joaquin Vanschoren, Jan N. van Rijn, Bernd Bischl, and Luis Torgo. OpenML: Networked science in machine learning. *SIGKDD Explorations*, 15(2):49–60, 2013. doi: 10.1145/2641190.2641198.

[58] Ashish Vaswani, Noam Shazeer, Niki Parmar, Jakob Uszkoreit, Llion Jones, Aidan N Gomez, Łukasz Kaiser, and Illia Polosukhin. Attention is all you need. In I. Guyon, U. Von Luxburg, S. Bengio, H. Wallach, R. Fergus, S. Vishwanathan, and R. Garnett, editors, *Advances in Neural Information Processing Systems*, volume 30, page 6000–6010, Red Hook, NY, USA, 2017. Curran Associates, Inc. ISBN 9781510860964.

[59] Alex X. Wang and Binh P. Nguyen. TTVAE: Transformer-based generative modeling for tabular data generation. *Artificial Intelligence*, 340:104292, 2025. ISSN 0004-3702. doi: <https://doi.org/10.1016/j.artint.2025.104292>.

[60] Yuxin Wang, Duanyu Feng, Yongfu Dai, Zhengyu Chen, Jimin Huang, Sophia Ananiadou, Qianqian Xie, and Hao Wang. HARMONIC: Harnessing LMs for tabular data synthesis and privacy protection. In A. Globerson, L. Mackey, D. Belgrave, A. Fan, U. Paquet, J. Tomczak, and C. Zhang, editors, *Advances in Neural Information Processing Systems*, volume 37, pages 100196–100212. Curran Associates, Inc., 2024.

[61] David S. Watson, Kristin Blesch, Jan Kapar, and Marvin N. Wright. Adversarial random forests for density estimation and generative modeling. In Francisco Ruiz, Jennifer Dy, and Jan-Willem van de Meent, editors, *Proceedings of The 26th International Conference on Artificial Intelligence and Statistics*, volume 206 of *Proceedings of Machine Learning Research*, pages 5357–5375. PMLR, 25–27 Apr 2023.

[62] W H Wolberg and O L Mangasarian. Multisurface method of pattern separation for medical diagnosis applied to breast cytology. *PNAS*, 87(23):9193–9196, 1990.

[63] Haiping Wu, Bin Xiao, Noel Codella, Mengchen Liu, Xiyang Dai, Lu Yuan, and Lei Zhang. CvT: Introducing convolutions to vision transformers. In *2021 IEEE/CVF International Conference on Computer Vision (ICCV)*, pages 22–31, 2021. doi: 10.1109/ICCV48922.2021.00009.

[64] Lei Xu, Maria Skoularidou, Alfredo Cuesta-Infante, and Kalyan Veeramachaneni. Modeling tabular data using conditional GAN. In H. Wallach, H. Larochelle, A. Beygelzimer, F. d’Alché-Buc, E. Fox, and R. Garnett, editors, *Advances in Neural Information Processing Systems*, volume 32, pages 7335–7345, Red Hook, NY, USA, 2019. Curran Associates, Inc.

[65] Hengrui Zhang, Jiani Zhang, Zhengyuan Shen, Balasubramaniam Srinivasan, Xiao Qin, Christos Faloutsos, Huzeifa Rangwala, and George Karypis. Mixed-type tabular data synthesis with score-based diffusion in latent space. In *The Twelfth International Conference on Learning Representations, ICLR 2024, Vienna, Austria, May 7-11, 2024*. OpenReview.net, 2024.

[66] Shihao Zhang, Linlin Yang, Michael Bi Mi, Xiaoxu Zheng, and Angela Yao. Improving deep regression with ordinal entropy. In *The Eleventh International Conference on Learning Representations, ICLR 2023, Kigali, Rwanda, May 1-5, 2023*. OpenReview.net, 2023.

- [67] Zilong Zhao, Aditya Kunar, Robert Birke, and Lydia Y. Chen. CTAB-GAN: Effective table data synthesizing. In Vineeth N. Balasubramanian and Ivor Tsang, editors, *Proceedings of The 13th Asian Conference on Machine Learning*, volume 157 of *Proceedings of Machine Learning Research*, pages 97–112. PMLR, 17–19 Nov 2021.
- [68] Zilong Zhao, Robert Birke, and Lydia Y. Chen. TabuLa: Harnessing language models for tabular data synthesis. *CoRR*, abs/2310.12746, 2023. doi: 10.48550/ARXIV.2310.12746. URL <https://doi.org/10.48550/arXiv.2310.12746>.
- [69] Zilong Zhao, Aditya Kunar, Robert Birke, Hiek Van der Scheer, and Lydia Y. Chen. CTAB-GAN+: enhancing tabular data synthesis. *Frontiers in Big Data*, 6, 2024. ISSN 2624-909X. doi: 10.3389/fdata.2023.1296508.

Algorithm 1 Training of TabTreeFormer

```
1: Input: Tabular dataset  $\mathbf{X}$  ( $n$  rows,  $m_d$  discrete features,  $m_c$  continuous features),  $s_0$  shared initial steps,  $s$  total training steps
2: Output: Fitted tree-based model  $\mathcal{T}$  and the leaf index matrices  $\mathbf{J}_1, \mathbf{J}_2$ , data tokenizer  $\mathcal{D}$ , and transformers  $\mathcal{G}_1, \mathcal{G}_2$ 
3:  $\mathcal{T} \leftarrow \text{TUNEANDFITTREEBASEDMODEL}(\mathbf{X})$   $\blacktriangleright$  Let  $T = \mathcal{T}.\text{N\_TREES}$ ,  $n_l = \mathcal{T}.\text{MAX\_N\_LEAVES}$ 
4:  $\mathbf{J} \leftarrow \mathcal{T}.\text{GETLEAFINDEX}(\mathbf{X})$   $\blacktriangleright$  Obtain leaf index matrix  $\mathbf{J} \in \mathbb{N}^{n \times T}$ 
5:  $\mathcal{D} \leftarrow \text{FITENCODER}(\mathbf{X})$   $\blacktriangleright n_c = \mathcal{D}.\text{MAX\_N\_CAT}$ ,  $n_b = \mathcal{D}.\text{MAX\_N\_BIN}$ ,  $n_q = \mathcal{D}.\text{MAX\_N\_QUANT}$ 
6:  $\tilde{\mathbf{X}} \leftarrow \mathcal{D}.\text{ENCODE}(\mathbf{X})$   $\blacktriangleright$  Get cat/bin/quant IDs  $\tilde{\mathbf{X}} \in \mathbb{N}^{n \times (m_d + 2m_c)}$ 
7:  $\mathbf{Z} \leftarrow \text{TOTOKENIDS}([\mathbf{J}; \tilde{\mathbf{X}}])$   $\blacktriangleright$  Convert these IDs to token IDs, add BOS, EOS
8:  $\mathcal{G} \leftarrow \text{INITIALZELM}(n_{\text{pos}} = 2 + T + m_d + 2m_c, n_{\text{vocab}} = 3 + n_l + n_c + n_b + n_q)$ 
 $\blacktriangleright$  Also initialize embedding layer on quantile tokens with ordinal relations
9: for  $i = 1, \dots, s_0$  do
10:    $\mathbf{B} \leftarrow \text{SAMPLEBATCH}(\mathbf{Z})$ 
11:    $\tilde{\mathbf{B}} \leftarrow \text{MASK}(\mathbf{B})$ 
12:    $\mathcal{G} \leftarrow \text{UPDATEGRADIENT}(\text{input} = \tilde{\mathbf{B}}, \text{target} = \mathbf{B})$ 
13: end for  $\blacktriangleright$  Prepare some non-overfitted trained weights
14:  $[\mathbf{J}_1, \mathbf{J}_2], [\mathbf{Z}_1, \mathbf{Z}_2] \leftarrow \text{EVENLYSPLIT}(\mathbf{J}, \mathbf{Z})$ 
15:  $\mathcal{G}_1, \mathcal{G}_2 \leftarrow \text{MAKECOPIES}(\mathcal{G}, 2)$ 
16: for  $j = 1, 2$  do
17:   for  $i = s_0 + 1, \dots, s$  do
18:      $\mathbf{B} \leftarrow \text{SAMPLEBATCH}(\mathbf{Z}_j)$ 
19:      $\tilde{\mathbf{B}} \leftarrow \text{MASK}(\mathbf{B})$ 
20:      $\mathcal{G}_j \leftarrow \text{UPDATEGRADIENT}(\text{input} = \tilde{\mathbf{B}}, \text{target} = \mathbf{B})$ 
21:     if  $\text{VALIDATEATSTEP}(i)$  then
22:        $\ell \leftarrow \text{COMPUTELOSS}(\text{input} = \text{MASK}(\mathbf{Z}_{1-j}), \text{target} = \mathbf{Z}_{1-j})$   $\blacktriangleright$  Compute validation loss
23:       if  $\text{METEARLYSTOPCRITERION}(\ell)$  then
24:          $i \leftarrow s$   $\blacktriangleright$  Early stop
25:       end if
26:     end if
27:   end for
28: end for
```

A Supplementary TabTreeFormer Model Description and Details

Section A.1 provides the full end-to-end training and generation process, and Section A.2-A.4 provide detailed model setup of core components.

A.1 End-to-end TabTreeFormer Pipeline

As a supplementary of Fig. 2 on the overall process of TabTreeFormer, and the textual description in Section 3, we provide the full end-to-end pseudocode in this section. Algorithm 1 and Algorithm 2 describe the end-to-end training and generation process of TabTreeFormer respectively.

A.2 Tree-based Model

A.2.1 Hyperparameter Tuning

For the tree-based classifier or regressor, we use Optuna [1] to tune the hyperparameters of LightGBM [31] using the training data. If the dataset has a designated target column, which is the case for all our experimented datasets, the model is trained to predict that column. Otherwise, a random column can be the target. Then, fit the model with the selected hyperparameters for TabTreeFormer.

The hyperparameter space explored is

- **Learning Rate:** Logarithmic scale float in $[0.01, 0.3]$;
- **Number of Estimators:** Integers in $[50, 250]$ step 50;
- **Maximum Depth:** Integers in $[3, 10]$;
- **Number of Leaves:** Integers in $[20, 100]$ step 5;
- **Minimum Size per Leaf:** Integers in $[10, 50]$ step 5;
- **Feature Fraction:** Float in $[0.6, 1.0]$;
- **Bagging Fraction:** Float in $[0.6, 1.0]$;

Algorithm 2 Tabular data generation using TabTreeFormer

```
1: Input: Leaf index matrices  $\mathbf{J}_1, \mathbf{J}_2$ , data tokenizer  $\mathcal{D}$ , transformer-based language models  $\mathcal{G}_1, \mathcal{G}_2$ , and  
number of rows generate  $n'$   
2:  $n_1, n_2 \leftarrow \lfloor n'/2 \rfloor, \lceil n'/2 \rceil$  ▶ Assign number of rows for each network  
3: Output: Synthetic tabular dataset  $\mathbf{X}'$   
4: for  $j = 1, 2$  do  
5:    $\mathbf{J}'_j \leftarrow \text{SAMPLE}(\mathbf{J}_j, n_j)$   
6:    $\mathbf{Z}'_j \leftarrow \text{MASK}(\text{TOTOKENIDS}(\mathbf{J}'_j))$  ▶ Prepare tokens as prompts  
7:    $\tilde{\mathbf{X}}'_j \leftarrow \mathcal{G}_j.\text{GENERATE}(\text{partial\_input} = \mathbf{Z}'_j)$   
8:    $\mathbf{X}'_j \leftarrow \mathcal{D}.\text{DECODE}(\tilde{\mathbf{X}}'_j)$   
9: end for  
10:  $\mathbf{X}' \leftarrow \text{COMBINE}(\mathbf{X}'_1, \mathbf{X}'_2)$ 
```

Table 7: Hyperparameter configuration of TabTreeFormer of different sizes.

TabTreeFormer	S	L
Approx. #Params (in M)	5	40
hidden state dimensions	256	768
inner feed-forward layer dimensions	1024	3072
number of attention heads per layer	8	12

- **L1 Regularization:** Float in $[0.0, 10.0]$;
- **L2 Regularization:** Float in $[0.0, 10.0]$.

Optimization was performed over 50 trials using 3-fold cross-validation, performance evaluated based on weighted F1 for classification and (negative) mean squared error for regression.

A.2.2 Leaf Index Matrix

In the subsequent steps of TabTreeFormer, leaf index matrix \mathbf{J} of the real data \mathbf{X} is computed. The indexing order of trees and their leaves used in the subsequent steps are directly taken from the fitted tree-based model. The leaf index matrix is essentially the result of `.apply` function for most tree-based models in `sklearn`.

A.3 Tokenization

For K-Means and quantile quantization, we use `sklearn.preprocessing.KBinsDiscretizer` with strategy “kmeans” and “quantile” respectively. For categorical values, we use `sklearn.preprocessing.OrdinalEncoder`.

In cases where the number of distinct values expected to be kept is way larger than typical natural language models’ vocabulary size, two or more consecutive quantile quantizers may be used, where subsequent quantizers are used to quantize the values in the same quantile as suggested by previous quantizers. Thus, with q quantizers, a total of Q^q values can be represented, which is sufficient to cover most practical cases. In this paper, we present $Q = 1000$ as sufficient precision for simplicity.

A.4 Transformer

A.4.1 Model Configuration

For the language model, we use Distill-GPT2 [50], based on the GPT2 architecture [48], with several modifications. The vocabulary size and maximum sequence length are adjusted based on the dataset, and the values are likely much lower than the requirement for natural language models. For example, if $n_l = 200, n_c = 20, n_b = K = 10, n_q = Q = 1000$, then $V = 1233$, and if $T = 200, m_d = 10, m_c = 10$, then $L = 222$, while natural language models typically have $V > 30000, L > 1000$.

In this paper, we present 3 versions of TabTreeFormer of different sizes. Table 7 shows their details. The model sizes are obtained for diabetes [54] dataset. Actual values may vary based on the fitted tree-based model and dataset.

A.4.2 Token Sequence Construction

The tokens in Table 1 are conceptual tokens. When converting the leaf, category, K-Means bin, and quantile IDs into token IDs in actual implementation, we do not explicitly make the textual tokens, but instead, directly add corresponding token type’s offset.

A.4.3 Masking

Instead of using a fixed mask ratio, we apply varying mask ratios to enhance the diversity of training data. Tree-related tokens (yellow section in Fig. 2) are masked with a ratio sampled uniformly from $[0.5, 0.75]$, while actual value tokens (blue section in Fig. 2) are masked with a ratio sampled uniformly from $[0.25, 0.5]$. In the no-mask (NM) version, we set both mask ratios to be constant 0.

To ensure that the quantile token is always masked if its corresponding K-Means bin token is masked within the same numeric column, we first generate a random mask. If a violation is detected (i.e., the K-Means bin token is unmasked while the quantile token is masked), we swap the mask values of these two positions. This approach ensures that masks are generated both efficiently and accurately.

A.4.4 Training Configuration

The reduced model size allows for a significantly larger batch size compared to typical natural language models. We use a batch size of 128 per device, reduce by half in case of CUDA OOM³, and train for up to 5,000 steps ($s = 5,000$ in Algorithm 1) with a learning rate of 5×10^{-4} in FP16 precision, utilizing the Hugging Face Trainer. Early stopping may be triggered by validation loss with a patience of 3 every 100 steps. Patience is set to 100 in the NM version. The initial training on both splits (Line 9-13 in Algorithm 1) is trained with the number of steps (s_0) set to the smaller of the number of steps required for 20 epochs and 1/10 of s .

A.4.5 Model Inference

Tree-leaf tokens from real data after masking are used as prompts for generation. Values of categorical columns are more likely to be memorized than numeric values by our ordinal learning method. Therefore, we apply a higher temperature to the tokens for categorical values and a lower one to the tokens for numeric values. In particular, we set the temperature for categorical tokens to be 2.0 and numeric tokens, including bin and quantile tokens, to be 1.0. In the NM version, we set the temperatures to be 0.2 and 0.1 respectively.

Recall that a set of valid tokens can be pre-determined at each position. Formally, let p_i be the corresponding feature index for the i -th token from data tokenizer, and R_i indicates the type of this token. For example, in Fig. 2, $p_1 = 1, p_2 = 1, p_3 = 2, R_1 = \text{bin}, R_2 = \text{quant}, R_3 = \text{cat}$. Then, let \mathcal{V}_i be the set of tokens allowed at position $i \in \{1, 2, \dots, L\}$, we have Equation 7.

$$\mathcal{V}_i = \begin{cases} \{[\text{BOS}]\} & \text{if } i = 1 \\ \{[\text{leaf1}], \dots, [\text{leaf}(l_{i-1})]\} & \text{if } 2 \leq i \leq T + 1 \\ \{[\text{bin1}], \dots, [\text{bin}(b_{p_{i-T-1}})]\} & \text{if } T + 2 \leq i \leq L - 1 \text{ and } R_{i-T-1} = \text{bin} \\ \{[\text{quant1}], \dots, [\text{quant}(q_{p_{i-T-1}})]\} & \text{if } T + 2 \leq i \leq L - 1 \text{ and } R_{i-T-1} = \text{quant} \\ \{[\text{cat1}], \dots, [\text{cat}(b_{p_{i-T-1}})]\} & \text{if } T + 2 \leq i \leq L - 1 \text{ and } R_{i-T-1} = \text{cat} \\ \{[\text{EOS}]\} & \text{if } i = L \end{cases} \quad (7)$$

Valid tokens for a specific position is enforced by setting the logits of invalid tokens at the position to negative infinity before sampling.

B Supplementary Quantile Embeddings Explanation and Analysis

B.1 Preliminaries: Function-Generated Positional Embeddings

While positional embeddings can also be a learned embedding like word tokens, Vaswani et al. [58] found that its performance is not necessarily significantly better than function-generated positional

³Among all $10 \times 3 = 30$ experiments, TabTreeFormer-L hits CUDA OOM in one experiment, and no other TabTreeFormer experiments had memory issues with this batch size.

embeddings. Moreover, function-generated embeddings allow the model to extrapolate positional information in sentences longer than those in the training corpora.

The typical functions to generate positional embeddings written in a similar format as Equation 3 (expressed in i and d) are shown in Equation 8 [58].

$$PE_{id} = \begin{cases} \sin\left(\frac{i}{10000^{\frac{d}{D}}}\right) & \text{if } 2 \mid i \\ \cos\left(\frac{i}{10000^{\frac{d-1}{D}}}\right) & \text{if } 2 \nmid i \end{cases} \quad (8)$$

The functions are essentially sine and cosine functions, where the frequency is controlled by the dimension indices. Using these periodic functions is particularly suitable for positional embeddings, which focus more on relative differences than absolute differences.

B.2 Choice of the Core Generator Function for Quantile Embeddings

Periodic functions are proper generator functions for positional embeddings because of the relative nature of positions. Similarly, due to the absolute and monotonic nature of quantile values, monotonic functions are more suitable for the generator functions for quantile embeddings.

The simplest of monotonic functions are linear functions, but they suffer from the following problems:

- To obtain different linear functions at different embedding dimensions, the slopes and intercepts need to be changed. However, in order for the embedded values to fall in a reasonable range (no extremely large or small values), the choice of proper slopes and intercepts becomes very limited, which hurts the diversity between different embedding dimensions. This significantly downgrades the effect of having different embedding dimensions.
- Having linear functions in all dimensions means that different dimensions are in strict linear relations to one another. Note that transformers are heavily dependent on linear projections. In particular, the input embeddings are linearly projected to Q, K, V vectors of the first attention layer. Therefore, universal linear relations among all embedded dimensions would degenerate the power of the first few layers of the network, which is an undesired outcome.

Therefore, besides being monotonic, we also require the generator function to be non-linear and have a controlled range (so ideally bounded). In this paper, we choose sigmoid, a simple function that satisfies the non-linear monotonic and bounded requirements. Nevertheless, we also note that other functions satisfying the requirements may also be used, such as tanh, softsign, and piece-wise linear functions.

B.3 Construction of Quantile Embeddings

For the standard sigmoid function $\text{sigmoid}(x) = \frac{1}{1+e^{-x}}$, we consider the range $[-2, 2]$ as the core range of x that has non-trivial changes of values (see Fig. 12). To project the total Q quantile tokens on this core range, we need to scale and shift the quantile ID i to $4\left(\frac{i}{Q} - \frac{1}{2}\right)$ (recall Equation 3).

The scale factor S_d (recall Equation 1) controls how the core range is distributed over the total Q quantile tokens. For a given scale factor value $s \in \mathbb{N}^+$, we assign $2s$ embedded dimensions with different offsets. More dimensions are assigned to larger scale factors because of the smaller number of tokens having transformed input values falling in the core range of the sigmoid function. Thus, the vector of S_d for $d = 0, 1, \dots, D-1$ is constructed by `repeat(arange(n)+1, 2*(arange(n)+1))[:D]` of a large enough n .

Proposition 1. *Equation 1 is a closed form of the scale factor construction above (`repeat(arange(n)+1, 2*(arange(n)+1))[:D]`).*

Proof. The construction means that for scale factor value $s \in \mathbb{N}^+$ starting from 1, the same value repeats $2s$ times. Let S'_d be the value by the construction, and $\mathcal{J}(s) = \{d \mid S'_d = s\}$, then $\mathcal{J}(s)$ must be a set of consecutive integers, and

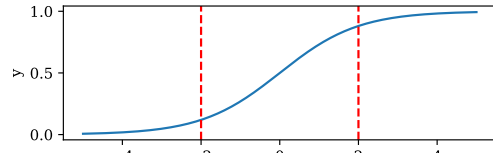


Figure 12: Sigmoid function $y = \text{sigmoid}(x)$. The red vertical dashed lines highlight the range $x \in [-2, 2]$ where the changes of values are considered non-trivial.

$$\min \mathcal{J}(s) = \sum_{i=1}^{s-1} 2s = (1+s-1)(s-1) = s^2 - s \quad (9)$$

$$\max \mathcal{J}(s) = \min \mathcal{J}(s) + 2s - 1 = s^2 + s - 1 \quad (10)$$

Let $\hat{S}_d = \frac{1+\sqrt{1+4d}}{2}$, then $S_d = \lfloor \hat{S}_d \rfloor$. Then, by $s \geq 1$,

$$\hat{S}_{\min \mathcal{J}(s)} = \hat{S}_{s^2-s} = \frac{1 + \sqrt{1 + 4(s^2 - s)}}{2} = \frac{1 + \sqrt{(2s-1)^2}}{2} = \frac{1 + |2s-1|}{2} = s \quad (11)$$

$$\begin{aligned} \hat{S}_{\max \mathcal{J}(s)} &= \hat{S}_{s^2+s-1} = \frac{1 + \sqrt{1 + 4(s^2 + s - 1)}}{2} = \frac{1 + \sqrt{(2s+1)^2 - 4}}{2} \\ &< \frac{1 + \sqrt{(2s+1)^2}}{2} = \frac{1 + |2s+1|}{2} = s+1 \end{aligned} \quad (12)$$

Note that \hat{S}_d is monotonically increasing with respect to d , then we must have

$$\hat{S}_d \in [s, s+1], \forall d \in \mathcal{J}(s) \quad (13)$$

This concludes to

$$S_d = \lfloor \hat{S}_d \rfloor = s \quad (14)$$

Given $s \in \mathbb{N}^+$, then $S_d \in \mathbb{N}^+$. \square

For embedding dimensions corresponding to the same scale factor S_d , we apply evenly distributed offsets in $[-2S_d, 2S_d]$, where the constant factors $-2, 2$ also come from the core range $x \in [-2, 2]$. Thus, the vector of offsets O_d for $d = 0, 1, \dots, D-1$ is constructed by `concat(linspace(-2*x, 2*x, 2*x) for x in (arange(n)+1))[:D]`.

Proposition 2. *Equation 2 is a closed form of the offset construction above (`concat(linspace(-2*x, 2*x, 2*x) for x in (arange(n)+1))[:D]`).*

Proof. The x in the construction is s in the previous proof. Let the i -th offset value with $S_d = s$ be o_{si} by the construction. Then we have $i \in [0, 2s]$ and

$$o_{si} = -2s + i \cdot \frac{2s - (-2s)}{2s - 1} = \frac{-4s^2 + 2s + 4si}{2s - 1} = \frac{2s(-2s + (2i + 1))}{2s - 1} \quad (15)$$

Let O'_d be the d -th value in the constructed offset value, regardless of scale factor, then substitute with Equation 15, 9 and 2,

$$O'_d = o_{S_d(d-\min \mathcal{J}(S_d))} = \frac{2S_d(-2S_d + (2(d - S_d^2 + S_d) + 1))}{2S_d - 1} \quad (16)$$

$$= \frac{-4S_d^3 + (4d + 2)S_d}{2S_d - 1} = O_d \quad (17)$$

Furthermore, $o_{si} \in [-2s, 2s]$, so $O_d \in [-2S_d, 2S_d]$. \square

Applying the sigmoid function on the quantile IDs with the scale factors and offsets, we obtain the quantile embedding value generators in Equation 3.

B.4 Comparison between Quantile Embeddings and Positional Embeddings

Table 8 shows a summary of the comparison between the proposed quantile embeddings and the typical function-generated positional embeddings. The two function-generated embeddings are also visualized in Fig. 13.

Table 8: Comparison between the proposed function-generated quantile and typical function-generated positional embeddings for transformers [58].

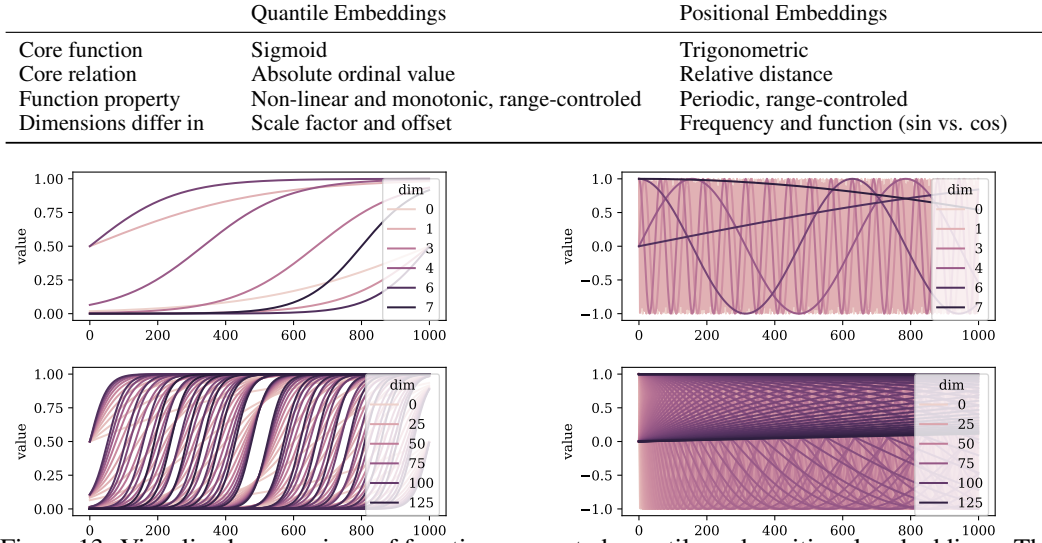


Figure 13: Visualized comparison of function-generated quantile and positional embeddings. The x -axis represents $i \in \{0, 1, \dots, Q-1\}$ (where $Q = 1000$) and y -axis represents the corresponding embedded values. Different colors of lines represent different embedded dimensions. **Left:** quantile embeddings (Equation 3), **Right:** positional embeddings (Equation 8), **Top:** $D = 8$, **Bottom:** $D = 128$.

B.5 Proof of Theorem 2

Proof. For simplicity of symbols, let $q_{id} = QE_{id}$. By Equation 3, $q_{id} = \text{sigmoid}(k_d i + b_d)$ for some $k_d \in \mathbb{R}^+$, $b_d \in \mathbb{R}$. Note that sigmoid is strictly monotonically increasing, and the linear function $k_d i + b_d$ with $k_d > 0$ is also strictly monotonically increasing concerning i . Thus, q_{id} is strictly monotonically increasing with respect to i .

If $|i - j| < |i - k|$, then $|q_{id} - q_{jd}| < |q_{id} - q_{kd}|, \forall d \in \{0, 1, \dots, D-1\}$, by the monotonicity of q_{id} with respect to i and triangle inequality. Then, by the strictly increasing monotonicity of $f(x) = x^p$ and $f(x) = x^{\frac{1}{p}}$ for $p \geq 1$ on $x \in \mathbb{R}^+ \cup \{0\}$ and by the monotonicity of the sum of monotonic functions, we must have

$$\|\mathbf{q}_i - \mathbf{q}_j\|_p = \left(\sum_{d=0}^{D-1} |q_{id} - q_{jd}|^p \right)^{\frac{1}{p}} < \left(\sum_{d=0}^{D-1} |q_{id} - q_{kd}|^p \right)^{\frac{1}{p}} = \|\mathbf{q}_i - \mathbf{q}_k\|_p \quad (18)$$

and by the monotonicity of the maximum of monotonic functions, we must have

$$\|\mathbf{q}_i - \mathbf{q}_j\|_\infty = \max_{0 \leq d < D} |q_{id} - q_{jd}| < \max_{0 \leq d < D} |q_{id} - q_{kd}| = \|\mathbf{q}_i - \mathbf{q}_k\|_\infty \quad (19)$$

Therefore, if $|i - j| < |i - k|$, then $\|\mathbf{q}_i - \mathbf{q}_j\|_p < \|\mathbf{q}_i - \mathbf{q}_k\|_p$.

In the inverse direction, we prove the contrapositive. If $|i - j| \geq |i - k|$, then $|q_{id} - q_{jd}| \geq |q_{id} - q_{kd}|, \forall d \in \{0, 1, \dots, D-1\}$. Next, by similar monotonic arguments above, we must have

$$\|\mathbf{q}_i - \mathbf{q}_j\|_p = \left(\sum_{d=0}^{D-1} |q_{id} - q_{jd}|^p \right)^{\frac{1}{p}} \geq \left(\sum_{d=0}^{D-1} |q_{id} - q_{kd}|^p \right)^{\frac{1}{p}} = \|\mathbf{q}_i - \mathbf{q}_k\|_p \quad (20)$$

and

$$\|\mathbf{q}_i - \mathbf{q}_j\|_\infty = \max_{0 \leq d < D} |q_{id} - q_{jd}| \geq \max_{0 \leq d < D} |q_{id} - q_{kd}| = \|\mathbf{q}_i - \mathbf{q}_k\|_\infty \quad (21)$$

The above shows that if $|i - j| \geq |i - k|$, then $\|\mathbf{q}_i - \mathbf{q}_j\|_p \geq \|\mathbf{q}_i - \mathbf{q}_k\|_p$. Therefore, if $\|\mathbf{q}_i - \mathbf{q}_j\|_p < \|\mathbf{q}_i - \mathbf{q}_k\|_p$, then $|i - j| < |i - k|$.

Summarizing the above, we have $|i - j| < |i - k|$ if and only if $\|\mathbf{q}_i - \mathbf{q}_j\|_p < \|\mathbf{q}_i - \mathbf{q}_k\|_p$, and the conclusion holds for any p . \square

Remark 1. According to the proof, any strictly monotonically increasing core function, not restricted to sigmoid, makes Theorem 2 hold.

Remark 2. Any monotonically increasing core function, including non-strictly monotonic ones, makes the “if” direction of Theorem 2 hold, with no guarantee of the “only if” direction (the two p -norm distances can be equal).

C Supplementary Loss Function Explanation and Analysis

C.1 Proof of Lemma 1

Proof. Firstly, note that $\frac{\partial w_{ti}}{\partial z_j} = 0, \forall i, j \in \{1, \dots, V\}$, by independence between the two. Also mind that $w_{ti} > 0, \forall i \in \{1, \dots, V\}$.

$$\begin{aligned} \frac{\partial \mathcal{L}_{\text{oce}}(\mathbf{z}, t)}{\partial z_t} &= -\frac{\sum_{i=1}^V w_{ti} e^{z_i}}{w_{tt} e^{z_t}} \cdot \frac{w_{tt} e^{z_t} \sum_{i=1}^V w_{ti} e^{z_i} - w_{tt} e^{z_t} \cdot w_{tt} e^{z_t}}{\left(\sum_{i=1}^V w_{ti} e^{z_i}\right)^2} \\ &= -\frac{\sum_{i=1}^V w_{ti} e^{z_i} - w_{tt} e^{z_t}}{\sum_{i=1}^V w_{ti} e^{z_i}} < 0 \end{aligned} \quad (22)$$

$$\frac{\partial \mathcal{L}_{\text{oce}}(\mathbf{z}, t)}{\partial z_i} = -\frac{\sum_{i=1}^V w_{ti} e^{z_i}}{w_{tt} e^{z_t}} \cdot \frac{-w_{ti} e^{z_i} \cdot w_{tt} e^{z_t}}{\left(\sum_{i=1}^V w_{ti} e^{z_i}\right)^2} = \frac{w_{ti} e^{z_i}}{\sum_{i=1}^V w_{ti} e^{z_i}} > 0 \quad (23)$$

Thus, $\mathcal{L}_{\text{oce}}(\mathbf{z}, t)$ is optimized (minimized) when $z_t \rightarrow \infty, z_i \rightarrow -\infty (t \neq i)$. \square

C.2 Proof of Theorem 3

Proof. Express \mathcal{L}_{oce} and \mathcal{L}_{ce} using \mathbf{p} , we have

$$\begin{aligned} \mathcal{L}_{\text{ce}}(\mathbf{z}, t) &= -\log p_t \\ \mathcal{L}_{\text{oce}}(\mathbf{z}, t) &= -\log \frac{w_{tt} e^{z_t}}{\sum_{i=1}^V w_{ti} e^{z_i}} = -\log \frac{w_{tt} \cdot \frac{e^{z_t}}{\sum_{i=1}^V e^{z_i}}}{\sum_{i=1}^V w_{ti} \cdot \frac{e^{z_i}}{\sum_{j=1}^V e^{z_j}}} = -\log \frac{w_{tt} p_t}{\sum_{i=1}^V w_{ti} p_i} = -\log \frac{w_{tt} p_t}{D(\mathbf{z})} \end{aligned} \quad (24)$$

By $\mathcal{L}_{\text{ce}}(\mathbf{z}, t) = \mathcal{L}_{\text{ce}}(\mathbf{z}^*, t)$, we have $p_t = p_t^*$. Given $D(\mathbf{z}) < D(\mathbf{z}^*)$, we must have $\mathcal{L}_{\text{oce}}(\mathbf{z}, t) < \mathcal{L}_{\text{oce}}(\mathbf{z}^*, t)$. \square

C.3 Detailed Explanations and Analysis of the Weight Function (Equation 6)

Recall the function of weight given the target token and current token in Equation 6. This section will provide detailed explanations and analysis of it.

The exponential term comes from the intuition that the difference between closer quantiles is much more significant than the difference between farther quantiles. Some scaling and shifting is applied on the exponential term. Fig. 14 illustrates the relationship between w_{ti} and i under varying values of σ and m . The parameter σ primarily governs the width around the target token where the weights are significantly altered; larger σ values result in a broader

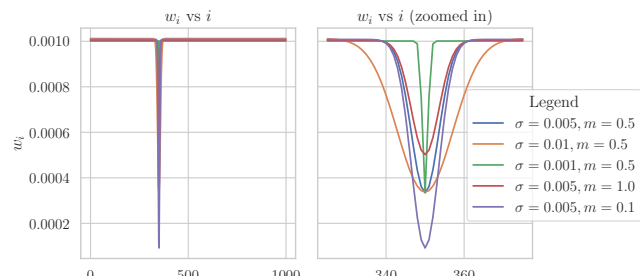


Figure 14: The relation of weights w_{ti} (normalized so that $\|\mathbf{w}\| = 1$ for visualization purpose) to token index i , with vocabulary size $V = 1000$, and target token $t = 350$.

Table 9: Datasets used in experiments. #R, #F, #N, and #C represents the number of rows, features (including target column), numeric features, and categorical features respectively. The task can be classification, denoted “clf” followed by the number of classes in the bracket, and regression, denoted “reg”. Aliases in bracket in “Name” column show the names used in this paper.

Name	#R	#F	#N	#C	Task
adult [33]	48842	15	2	13	clf(2)
bank-marketing (bank) [39]	45211	17	7	10	clf(2)
boston [23]	506	14	12	2	reg
breast-w (breast) [62]	699	10	9	1	clf(2)
credit-g (credit) [26]	1000	21	7	14	clf(2)
diabetes [54]	768	9	8	1	clf(2)
iris [17]	150	5	4	1	clf(3)
qsar-biodeg (qsar) [37]	1055	42	41	1	clf(2)
wdbc [56]	569	31	30	1	clf(2)

width. In contrast, m dictates the intensity of the weight modification, with smaller m values leading to more pronounced changes in weight.

C.4 Overall Loss Computation

Concerning the combination of valid quantile tokens and other non-quantile tokens, let valid quantile tokens have IDs in the range $[Q_s, Q_e]$. The valid token group loss (for quantile tokens at this position) is defined by Equation 26 when $t \in [Q_s, Q_e]$.

$$\mathcal{L}_{\text{vg}}(\mathbf{z}, t) = -\log \frac{\sum_{i \in [Q_s, Q_e]} e^{z_i}}{\sum_{i=1}^V e^{z_i}} \quad (26)$$

In sum, Equation 27 expresses the loss function on one token.

$$\mathcal{L}(\mathbf{z}, t) = \begin{cases} \mathcal{L}_{\text{ce}}(\mathbf{z}, t) & \text{if } t \notin [Q_s, Q_e] \\ \mathcal{L}_{\text{oce}}(\mathbf{z}_{Q_s:Q_e}, t - Q_s) + \mathcal{L}_{\text{vg}}(\mathbf{z}, t) & \text{if } t \in [Q_s, Q_e] \end{cases} \quad (27)$$

Although the ordinal property also holds for K-Means bin IDs, we do not calculate the loss on them this way because the number of different bins is small, and we expect the model to predict the bins accurately.

D Experiment Setup Details

D.1 Experiment Environment

Experiments were conducted on a system running Ubuntu 22.04.1 LTS with kernel version 6.8.0. The machine featured a 13th Gen Intel Core i9-13900K CPU with 24 cores and 32 threads, capable of a maximum clock speed of 5.8 GHz. GPU computations were performed using a single NVIDIA GeForce RTX 4090 with 24 GB VRAM. The environment was set up with NVIDIA driver version 565.57.01 and CUDA 12.7.

D.2 Details on Datasets

Table 9 shows the details of the datasets we used. Datasets are downloaded by `sklearn.datasets.fetch_openml`, with the dataset name as input. Random splits of 8 : 2 of training and test sets are applied.

D.3 Baseline Choices and Implementation

For i) non-neural-network method (tree-based sampling), ii) GAN [18], iii) VAE [32], and iv) Diffusion [25], we choose one recent, representative, and well-performing (especially on MLE) model each: Forest Diffusion [30], CTAB-GAN+ [69], TTVAE [59], and TabSyn [65]. For auto-regressive and masked transformers, which are more aligned with our work, we include more works:

GReaT [5], REaLTabFormer [55], TabMT [22], TabuLa [68]. All of them will use a DistilGPT2 [50] as the transformer backbone except for TabMT [22], which has specific settings described in its paper.

Other large language model (LLM)-based methods, such as HARMONIC [60], are excluded from our comparison for fairer comparison because

- They usually require a good-quality dataset description, but we want to focus on the case without additional information besides the data per se.
- Their performance is dependent on a very large and good LLM. The improvement of the LLM model may be more important than the improvement of the tabular-specific design, but we want to showcase the effectiveness of tabular-specific designs instead of an LLM.

We use the Synthcity [47] implementation for GReaT [5]. Our benchmark code is adapted from Synthcity [47] too. We also include CTAB-GAN+ [69], REaLTabFormer [55], TabSyn [65], Forest Diffusion [30], TabuLa [68], and TTVAE [59] using their official code on GitHub or public SDK in the benchmark. TabMT [22] has no publicly available code, so we do experiments based on a reproduction of the model based on the paper’s description, so the model could be slightly different from that paper.

D.4 Machine Learning Efficacy (MLE) Metrics Implementation

Instead of running all models with fixed, typically default, parameters across all datasets, we perform hyperparameter tuning before reporting their performance. The tuning process follows the same methodology used to optimize the core tree-based model in TabTreeFormer, but with 30 trials per round of optimization.

For linear models, no hyperparameter tuning is performed, as they follow the classical definition without additional tunable parameters.

The hyperparameter space explored for random forest is

- **Number of Estimators:** Integers in [100, 300] step 50;
- **Maximum Depth:** Integers in [5, 20] step 5;
- **Minimum Samples Split:** Integers in [2, 10] step 2;
- **Minimum Size per Leaf:** Integers [1, 5];
- **Maximum Features:** Value in “sqrt”, “log2”, and NULL;
- **Bootstrap:** Enabled or disabled.

The hyperparameter space explored for XGBoost is:

- **Learning Rate:** Logarithmic scale float in [0.01, 0.3];
- **Number of Estimators:** Integers in [100, 300] step 50;
- **Maximum Depth:** Integers in [3, 10];
- **Minimum Child Weight:** Logarithmic scale float in [1.0, 10.0];
- **Minimum Split Loss Gamma:** Float in [0.0, 0.5];
- **Subsample Ratio:** Float in [0.5, 1.0];
- **Subsample Ratio of Columns by Tree:** Float in [0.5, 1.0];
- **L1 Regularization:** Float in [0.0, 10.0].

For all models, numeric values are standardized using standard scaling. Categorical values are one-hot encoded for linear models and label-encoded for random forest and XGBoost. To simplify the experiments, rows with missing values are excluded, as handling missing data is not the focus of this paper.

The reported performance for machine learning utility is measured using the weighted AUC-ROC for classification tasks and the R^2 score for regression tasks, so for all these scores, a larger value indicates a better performance. Each generator is trained and used to generate synthetic data of the same size as the training dataset three times for each dataset, and the summarized results of these runs are reported.

D.5 Fidelity Metrics Implementation

Fidelity metrics are calculated using SDMetrics [13]’s public SDK.

Table 10: Performance comparison between different models in terms of MLE. Classification tasks are evaluated by weighted AUC ROC scores, and regression tasks are evaluated by R^2 scores. The last row shows the average relative error versus real. The best scores and the second best scores are highlighted in bold with and without underscore, respectively. Equal values in the first 3 digits may be compared by the 4-th or 5-th digits.

Dataset	ML	Real	CTAB+ [69]	TTVAE [59]	TabSyn [65]	FD [30]	GReAT [5]	RTF [55]	TabMT [22]	TabuLa [68]	TTF-S	TTF-L	TTF-NP	
adult	LN	0.914	0.904 \pm 0.001	0.875 \pm 0.010	0.910 \pm 0.002	0.911 \pm 0.000	0.911 \pm 0.000	0.911 \pm 0.000	0.913 \pm 0.000	0.906 \pm 0.001	0.911 \pm 0.001	0.910 \pm 0.000		
	RF	0.910	0.902 \pm 0.002	0.869 \pm 0.011	0.905 \pm 0.003	0.908 \pm 0.000	0.909 \pm 0.000	0.907 \pm 0.002	0.888 \pm 0.002	0.901 \pm 0.001	0.905 \pm 0.000	0.903 \pm 0.002		
	XGB	0.914	0.905 \pm 0.001	0.870 \pm 0.012	0.910 \pm 0.003	0.912 \pm 0.001	0.911 \pm 0.000	0.912 \pm 0.001	0.911 \pm 0.001	0.889 \pm 0.005	0.906 \pm 0.001	0.911 \pm 0.001	0.909 \pm 0.001	
bank	LN	0.907	0.901 \pm 0.002	0.885 \pm 0.004	0.900 \pm 0.005	0.903 \pm 0.001	0.907 \pm 0.000	0.904 \pm 0.000	0.862 \pm 0.005	0.906 \pm 0.001	0.906 \pm 0.000	0.906 \pm 0.000	0.901 \pm 0.000	
	RF	0.930	0.902 \pm 0.002	0.884 \pm 0.003	0.907 \pm 0.006	0.917 \pm 0.001	0.907 \pm 0.001	0.913 \pm 0.001	0.886 \pm 0.011	0.923 \pm 0.004	0.913 \pm 0.002	0.918 \pm 0.001	0.921 \pm 0.003	
	XGB	0.936	0.906 \pm 0.000	0.877 \pm 0.011	0.913 \pm 0.007	0.920 \pm 0.001	0.910 \pm 0.001	0.918 \pm 0.002	0.892 \pm 0.007	0.925 \pm 0.003	0.919 \pm 0.002	0.925 \pm 0.003	0.926 \pm 0.002	
boston	LN	0.590	0.264 \pm 0.034	0.000 \pm 0.078	0.533 \pm 0.036	0.542 \pm 0.016	0.397 \pm 0.000	0.529 \pm 0.028	0.409 \pm 0.015	0.484 \pm 0.069	0.525 \pm 0.035	0.575 \pm 0.011	0.591 \pm 0.000	
	RF	0.662	0.129 \pm 0.015	0.124 \pm 0.068	0.658 \pm 0.025	0.608 \pm 0.008	0.281 \pm 0.000	0.584 \pm 0.006	0.439 \pm 0.096	0.589 \pm 0.050	0.597 \pm 0.038	0.694 \pm 0.041	0.683 \pm 0.016	
	XGB	0.701	0.097 \pm 0.078	0.211 \pm 0.121	0.647 \pm 0.017	0.604 \pm 0.024	0.277 \pm 0.014	0.578 \pm 0.056	0.446 \pm 0.115	0.615 \pm 0.069	0.594 \pm 0.061	0.665 \pm 0.026	0.691 \pm 0.023	
breast	LN	0.985	0.913 \pm 0.091	0.963 \pm 0.006	0.987 \pm 0.001	0.986 \pm 0.002	0.985 \pm 0.000	0.987 \pm 0.002	0.983 \pm 0.004	0.985 \pm 0.001	0.981 \pm 0.005	0.987 \pm 0.002	0.984 \pm 0.004	
	RF	0.985	0.968 \pm 0.012	0.979 \pm 0.004	0.981 \pm 0.002	0.975 \pm 0.005	0.979 \pm 0.004	0.980 \pm 0.000	0.978 \pm 0.002	0.976 \pm 0.005	0.978 \pm 0.001	0.983 \pm 0.002	0.984 \pm 0.002	
	XGB	0.984	0.958 \pm 0.025	0.970 \pm 0.009	0.987 \pm 0.001	0.984 \pm 0.002	0.982 \pm 0.002	0.982 \pm 0.002	0.979 \pm 0.002	0.982 \pm 0.002	0.983 \pm 0.003	0.982 \pm 0.003		
credit	LN	0.836	0.538 \pm 0.093	0.500 \pm 0.000	0.780 \pm 0.017	0.827 \pm 0.010	0.665 \pm 0.000	0.801 \pm 0.006	0.773 \pm 0.038	0.814 \pm 0.016	0.816 \pm 0.020	0.755 \pm 0.011	0.834 \pm 0.001	
	RF	0.837	0.505 \pm 0.097	0.500 \pm 0.000	0.791 \pm 0.012	0.819 \pm 0.009	0.722 \pm 0.014	0.820 \pm 0.010	0.763 \pm 0.019	0.805 \pm 0.019	0.781 \pm 0.026	0.741 \pm 0.027	0.813 \pm 0.026	
	XGB	0.844	0.509 \pm 0.084	0.500 \pm 0.000	0.795 \pm 0.014	0.836 \pm 0.010	0.739 \pm 0.006	0.797 \pm 0.039	0.761 \pm 0.030	0.817 \pm 0.020	0.796 \pm 0.011	0.764 \pm 0.014	0.826 \pm 0.026	
diabetes	LN	0.884	0.817 \pm 0.028	0.880 \pm 0.003	0.883 \pm 0.006	0.885 \pm 0.001	0.858 \pm 0.000	0.878 \pm 0.003	0.855 \pm 0.014	0.876 \pm 0.007	0.890 \pm 0.010	0.886 \pm 0.001	0.843 \pm 0.058	
	RF	0.869	0.802 \pm 0.014	0.849 \pm 0.004	0.844 \pm 0.012	0.856 \pm 0.012	0.824 \pm 0.012	0.841 \pm 0.010	0.845 \pm 0.009	0.863 \pm 0.003	0.855 \pm 0.014	0.859 \pm 0.010	0.814 \pm 0.073	
	XGB	0.867	0.811 \pm 0.005	0.851 \pm 0.001	0.847 \pm 0.009	0.846 \pm 0.012	0.831 \pm 0.003	0.849 \pm 0.010	0.840 \pm 0.009	0.857 \pm 0.009	0.852 \pm 0.015	0.848 \pm 0.017	0.811 \pm 0.085	
iris	LN	1.000	0.272 \pm 0.064	0.996 \pm 0.006	0.999 \pm 0.002	0.997 \pm 0.005	0.985 \pm 0.000	0.983 \pm 0.015	1.000 \pm 0.000	-	0.971 \pm 0.018	0.997 \pm 0.005	1.000 \pm 0.000	
	RF	1.000	0.396 \pm 0.099	0.992 \pm 0.012	1.000 \pm 0.000	1.000 \pm 0.000	0.993 \pm 0.005	0.993 \pm 0.005	-	0.999 \pm 0.002	0.988 \pm 0.017	0.967 \pm 0.047		
	XGB	1.000	0.211 \pm 0.042	0.999 \pm 0.002	1.000 \pm 0.000	1.000 \pm 0.000	0.998 \pm 0.003	1.000 \pm 0.000	-	1.000 \pm 0.000	1.000 \pm 0.000	0.999 \pm 0.001		
qsar	LN	0.906	0.716 \pm 0.085	0.669 \pm 0.120	0.867 \pm 0.012	0.881 \pm 0.005	0.673 \pm 0.000	0.880 \pm 0.003	0.887 \pm 0.005	0.868 \pm 0.034	0.874 \pm 0.013	0.876 \pm 0.006	0.907 \pm 0.000	
	RF	0.936	0.648 \pm 0.036	0.666 \pm 0.117	0.882 \pm 0.006	0.897 \pm 0.011	0.610 \pm 0.009	0.907 \pm 0.007	0.880 \pm 0.008	0.825 \pm 0.028	0.873 \pm 0.006	0.884 \pm 0.004	0.925 \pm 0.006	
	XGB	0.921	0.731 \pm 0.020	0.658 \pm 0.114	0.860 \pm 0.016	0.889 \pm 0.010	0.602 \pm 0.020	0.897 \pm 0.010	0.873 \pm 0.009	0.842 \pm 0.023	0.862 \pm 0.005	0.884 \pm 0.004	0.917 \pm 0.005	
wdbc	LN	0.993	0.929 \pm 0.053	0.976 \pm 0.019	0.992 \pm 0.001	0.993 \pm 0.002	0.979 \pm 0.000	0.988 \pm 0.003	0.984 \pm 0.006	-	0.980 \pm 0.007	0.979 \pm 0.007	0.993 \pm 0.000	
	RF	0.976	0.919 \pm 0.024	0.952 \pm 0.041	0.984 \pm 0.004	0.982 \pm 0.004	0.970 \pm 0.003	0.980 \pm 0.012	0.978 \pm 0.003	-	0.981 \pm 0.001	0.975 \pm 0.002	0.981 \pm 0.001	
	XGB	0.990	0.930 \pm 0.021	0.949 \pm 0.035	0.986 \pm 0.002	0.989 \pm 0.001	0.973 \pm 0.003	0.988 \pm 0.002	0.982 \pm 0.004	-	0.987 \pm 0.003	0.985 \pm 0.006	0.989 \pm 0.001	

D.6 Distance to Closest Record (DCR) Metrics Implementation

The way the DCR values are reported differ from paper to paper. Also, existing papers often report a value and claim some specific value to be an ideal value, overlooking the fact that better privacy usually sacrifices quality. Thus, in this paper, we instead apply a statistical test on DCR values to *validate* privacy-preserving capability of the models, instead of *evaluating* it, which is likely also more useful in practical privacy-preserving data sharing cases.

We compare the DCR to the real training dataset \mathbf{X} of a hold-out real dataset $\hat{\mathbf{X}}$ with a synthetic dataset of the same size \mathbf{X}' , and privacy-preserving means that DCRs calculated on the latter is not smaller than DCRs calculated on the former. We test this using Mann-Whitney U Test [36], with the null hypothesis H_0 being that the distance between $\hat{\mathbf{X}}$ and \mathbf{X} is greater than or equal to \mathbf{X}' and \mathbf{X} , and if the p -value is less than 0.05, \mathbf{X}' is closer to \mathbf{X} than $\hat{\mathbf{X}}$, implying a risk of privacy leakage.

The data is preprocessed by quantile transformation (at 1000 quantiles, which is the same number of bins for the quantile quantizer in TabTreeFormer) for numeric values and one-hot encoding for categorical values for distance calculation. Cosine distance (calculated using `sklearn`) is used to evaluate the distance between records. As a reference, we calculate the cosine distances between the real test set and the real train set, obtaining the minimum distance per record for the test set. Similarly, we compute the cosine distances between synthetic data (with the same number of rows as the real test set) and the real train set, and also obtain the minimum distances. These distances are compared with the reference values to assess the similarity and privacy-preserving characteristics of the synthetic data.

E Raw Experimental Results

E.1 Raw Synthetic Data Quality Results

The raw experiment results for MLE is shown in Table 10. Out of the 27 MLE scores, TabTreeFormer-NM is the best in 11, while the best baseline achieves the best in at most 4).

The raw experiment results for fidelity is shown in Table 11.

Table 11: Performance comparison between different models in terms of fidelity. The closer the values are to 1, the better the fidelity is. The best scores and the second best scores are highlighted in bold with and without underscore, respectively. Equal values in the first 3 digits may be compared by the 4-th or 5-th digits.

Dataset	Metric	CTAB+ [69]	TTVAE [59]	TabSyn [65]	FD [30]	GReaT [5]	RTF [55]	TabMT [22]	TabuLa [68]	TTF-S	TTF-L	TTF-NP
adult	Shape	0.964 \pm 0.005	0.852 \pm 0.024	0.977 \pm 0.011	0.986 \pm 0.000	0.929 \pm 0.000	0.962 \pm 0.001	0.974 \pm 0.003	0.975 \pm 0.000	0.951 \pm 0.002	0.957 \pm 0.003	0.921 \pm 0.003
	Trend	0.915 \pm 0.004	0.733 \pm 0.032	0.955 \pm 0.018	0.972 \pm 0.000	0.882 \pm 0.000	0.933 \pm 0.003	0.957 \pm 0.004	0.956 \pm 0.001	0.887 \pm 0.003	0.895 \pm 0.005	0.838 \pm 0.027
bank	Shape	0.965 \pm 0.002	0.875 \pm 0.009	0.983 \pm 0.005	0.970 \pm 0.001	0.915 \pm 0.000	0.967 \pm 0.001	0.969 \pm 0.009	0.983 \pm 0.000	0.927 \pm 0.003	0.935 \pm 0.003	0.932 \pm 0.001
	Trend	0.884 \pm 0.003	0.788 \pm 0.017	0.967 \pm 0.008	0.965 \pm 0.019	0.903 \pm 0.000	0.953 \pm 0.001	0.944 \pm 0.034	0.971 \pm 0.000	0.944 \pm 0.006	0.956 \pm 0.003	0.935 \pm 0.027
boston	Shape	0.850 \pm 0.003	0.663 \pm 0.023	0.893 \pm 0.003	0.895 \pm 0.002	0.916 \pm 0.000	0.942 \pm 0.004	0.835 \pm 0.009	0.861 \pm 0.030	0.843 \pm 0.006	0.855 \pm 0.003	0.863 \pm 0.000
	Trend	0.828 \pm 0.011	0.747 \pm 0.021	0.934 \pm 0.003	0.942 \pm 0.001	0.908 \pm 0.000	0.947 \pm 0.002	0.935 \pm 0.014	0.886 \pm 0.004	0.951 \pm 0.020	0.973 \pm 0.006	0.992 \pm 0.000
breast	Shape	0.775 \pm 0.024	0.498 \pm 0.052	0.813 \pm 0.005	0.835 \pm 0.006	0.728 \pm 0.000	0.753 \pm 0.014	0.841 \pm 0.048	0.814 \pm 0.003	0.866 \pm 0.022	0.848 \pm 0.010	0.758 \pm 0.116
	Trend	0.616 \pm 0.063	0.333 \pm 0.065	0.709 \pm 0.006	0.766 \pm 0.004	0.636 \pm 0.000	0.668 \pm 0.010	0.747 \pm 0.035	0.767 \pm 0.003	0.735 \pm 0.025	0.728 \pm 0.020	0.680 \pm 0.165
credit	Shape	0.937 \pm 0.013	0.555 \pm 0.001	0.932 \pm 0.007	0.960 \pm 0.001	0.932 \pm 0.000	0.944 \pm 0.003	0.955 \pm 0.004	0.970 \pm 0.002	0.941 \pm 0.000	0.946 \pm 0.010	0.992 \pm 0.008
	Trend	0.862 \pm 0.030	0.306 \pm 0.005	0.862 \pm 0.008	0.912 \pm 0.009	0.861 \pm 0.000	0.890 \pm 0.006	0.911 \pm 0.004	0.917 \pm 0.000	0.880 \pm 0.012	0.883 \pm 0.018	0.958 \pm 0.019
diabetes	Shape	0.923 \pm 0.006	0.887 \pm 0.017	0.955 \pm 0.007	0.943 \pm 0.003	0.881 \pm 0.000	0.943 \pm 0.004	0.946 \pm 0.004	0.975 \pm 0.002	0.928 \pm 0.007	0.919 \pm 0.014	0.806 \pm 0.212
	Trend	0.898 \pm 0.004	0.888 \pm 0.012	0.964 \pm 0.002	0.957 \pm 0.006	0.921 \pm 0.000	0.952 \pm 0.003	0.971 \pm 0.012	0.954 \pm 0.004	0.957 \pm 0.000	0.924 \pm 0.091	-
iris	Shape	0.822 \pm 0.022	0.885 \pm 0.008	0.893 \pm 0.003	0.901 \pm 0.004	0.870 \pm 0.000	0.906 \pm 0.017	0.895 \pm 0.007	-	0.886 \pm 0.011	0.883 \pm 0.019	0.839 \pm 0.029
	Trend	0.590 \pm 0.019	0.878 \pm 0.004	0.917 \pm 0.007	0.920 \pm 0.006	0.899 \pm 0.000	0.896 \pm 0.016	0.901 \pm 0.011	-	0.902 \pm 0.005	0.922 \pm 0.018	0.895 \pm 0.055
qsar	Shape	0.917 \pm 0.003	0.652 \pm 0.031	0.930 \pm 0.005	0.947 \pm 0.004	0.887 \pm 0.000	0.959 \pm 0.003	0.920 \pm 0.006	0.833 \pm 0.034	0.914 \pm 0.000	0.936 \pm 0.003	0.954 \pm 0.001
	Trend	0.863 \pm 0.007	0.610 \pm 0.059	0.914 \pm 0.009	0.898 \pm 0.011	0.855 \pm 0.005	0.890 \pm 0.007	0.923 \pm 0.004	0.792 \pm 0.008	0.896 \pm 0.010	0.935 \pm 0.008	0.956 \pm 0.001
wdbc	Shape	0.861 \pm 0.005	0.754 \pm 0.047	0.946 \pm 0.004	0.946 \pm 0.004	0.873 \pm 0.000	0.945 \pm 0.006	0.937 \pm 0.008	-	0.938 \pm 0.007	0.957 \pm 0.003	0.980 \pm 0.004
	Trend	0.866 \pm 0.007	0.817 \pm 0.049	0.976 \pm 0.002	0.962 \pm 0.001	0.896 \pm 0.000	0.954 \pm 0.001	0.943 \pm 0.001	-	0.960 \pm 0.002	0.966 \pm 0.006	0.994 \pm 0.002

Table 12: Performance comparison between different models in terms of DCR. p -values less than 0.05 is highlighted in red, indicating a high risk of privacy leakage.

Dataset		CTAB+ [69]	TTVAE [59]	TabSyn [65]	FD [30]	GReaT [5]	RTF [55]	TabMT [22]	TabuLa [68]	TTF-S	TTF-L	TTF-NP
adult	1.000 \pm 0.000	1.000 \pm 0.000	1.000 \pm 0.000	1.000 \pm 0.000	0.857 \pm 0.000	0.000 \pm 0.000	0.998 \pm 0.002	0.000 \pm 0.000	1.000 \pm 0.000	1.000 \pm 0.000	1.000 \pm 0.000	1.000 \pm 0.000
bank	1.000 \pm 0.000	1.000 \pm 0.000	1.000 \pm 0.000	0.394 \pm 0.082	1.000 \pm 0.000	1.000 \pm 0.000	1.000 \pm 0.000	0.000 \pm 0.000	1.000 \pm 0.000	1.000 \pm 0.000	1.000 \pm 0.000	1.000 \pm 0.000
boston	1.000 \pm 0.000	1.000 \pm 0.000	0.941 \pm 0.040	0.996 \pm 0.005	1.000 \pm 0.000	0.508 \pm 0.295	1.000 \pm 0.000	0.754 \pm 0.121	1.000 \pm 0.000	1.000 \pm 0.000	1.000 \pm 0.000	1.000 \pm 0.000
breast	1.000 \pm 0.000	1.000 \pm 0.000	0.231 \pm 0.105	0.003 \pm 0.001	0.082 \pm 0.000	0.002 \pm 0.001	0.259 \pm 0.064	0.000 \pm 0.000	0.990 \pm 0.012	0.996 \pm 0.005	0.332 \pm 0.470	-
credit	1.000 \pm 0.000	1.000 \pm 0.000	0.186 \pm 0.141	0.005 \pm 0.003	0.883 \pm 0.000	0.000 \pm 0.000	0.824 \pm 0.183	0.000 \pm 0.000	0.908 \pm 0.107	0.676 \pm 0.455	0.000 \pm 0.000	-
diabetes	1.000 \pm 0.000	0.753 \pm 0.288	0.029 \pm 0.024	0.000 \pm 0.000	0.998 \pm 0.000	0.077 \pm 0.076	0.876 \pm 0.149	0.000 \pm 0.000	0.867 \pm 0.158	0.603 \pm 0.310	0.333 \pm 0.471	-
iris	1.000 \pm 0.000	0.382 \pm 0.229	0.552 \pm 0.099	0.049 \pm 0.032	0.764 \pm 0.000	0.638 \pm 0.226	0.824 \pm 0.191	-	0.662 \pm 0.421	0.214 \pm 0.022	0.086 \pm 0.096	-
qsar	1.000 \pm 0.000	1.000 \pm 0.000	1.000 \pm 0.000	0.977 \pm 0.019	1.000 \pm 0.000	0.326 \pm 0.088	1.000 \pm 0.000	1.000 \pm 0.000	1.000 \pm 0.000	0.956 \pm 0.063	0.000 \pm 0.000	-
wdbc	1.000 \pm 0.000	1.000 \pm 0.000	0.092 \pm 0.111	0.000 \pm 0.000	1.000 \pm 0.000	0.998 \pm 0.001	1.000 \pm 0.000	-	0.967 \pm 0.021	0.261 \pm 0.179	0.000 \pm 0.000	-

E.2 Raw Privacy Results

The raw experiment results for DCR is shown in Table 12.

Notes on the No Mask (NM) Setting and Quality-privacy Dilemma. Summarizing the settings of the non-private version mentioned in Appendix A, TTF-NM in the paper means TTF-L model size with 0 masking rate and technically no early stopping. Such a setting makes the model prone to memorizing exact values in the training data, which is verified by our experiment results on DCR. Nevertheless, in a non-private setting, we regard this as permissible because privacy is not a concern.

In fact, for any model, synthetic data quality and its privacy are usually a dilemma, which is also consistent with our experiment results on different baselines. For example, the baseline model with the best MLE result overall is TabuLa [68], but it has a privacy issue in *all* datasets. In particular, we found that TabuLa has a DCR of 0 on more than 50% of the rows in many datasets, and a DCR of smaller than 1×10^{-6} on more than 80% of the rows. This indicates a severe memorization issue. In comparison, the worst-performing baseline model we tested, CTAB-GAN+ [69], does not have any issue with privacy according to the DCR scores.

Balance of Quality and Utility. Given the dilemma between quality and utility, the general objective of a tabular data generator should be a good balance between quality and privacy, instead of optimizing both simultaneously. Table 13 shows the MLE scores with privacy warnings. TabTreeFormer demonstrates a good balance.

E.3 Computation Time

The raw computation time of training and generation is shown in Table 14. TabTreeFormer trains two separate models for cross-validation, and training stops mainly by the validation loss, and occasionally by a maximum number of steps, so the relative training time compared to other auto-regressive transformer baselines is higher, but when trained on large datasets, TabTreeFormer shows its efficiency advantage more obviously.

Table 13: Raw MLE performances as shown in Table 10, but experiments with privacy risks as indicated in Table 12 highlighted and excluded from ranking. TTF-NM is not shown because it is not intended for a balanced objective. Baselines with more than half of the datasets having privacy concerns are removed.

Dataset	ML	real	CTAB+ [69]	TTVAE [59]	TabSyn [65]	GReaT [5]	RTF [55]	TabMT [22]	TTF-S	TTF-L
adult	LN	0.914	0.904 \pm 0.001	0.875 \pm 0.010	0.910 \pm 0.002	0.911\pm0.000	0.911\pm0.000	0.911 \pm 0.000	0.906 \pm 0.001	0.911\pm0.001
	RF	0.910	0.902 \pm 0.002	0.869 \pm 0.011	0.905 \pm 0.003	0.905 \pm 0.000	0.908\pm0.000	0.907\pm0.002	0.901 \pm 0.001	0.905\pm0.000
	XGB	0.914	0.905 \pm 0.001	0.870 \pm 0.012	0.910 \pm 0.003	0.911 \pm 0.000	0.912\pm0.001	0.911\pm0.001	0.906 \pm 0.001	0.911\pm0.001
bank	LN	0.907	0.901 \pm 0.003	0.885 \pm 0.004	0.900 \pm 0.005	0.907\pm0.000	0.904 \pm 0.000	0.862 \pm 0.005	0.906 \pm 0.000	0.906\pm0.000
	RF	0.930	0.902 \pm 0.002	0.884 \pm 0.009	0.907 \pm 0.006	0.907 \pm 0.001	0.913\pm0.001	0.886 \pm 0.011	0.913 \pm 0.002	0.918\pm0.001
	XGB	0.936	0.906 \pm 0.000	0.877 \pm 0.011	0.913 \pm 0.001	0.910 \pm 0.001	0.918 \pm 0.002	0.892 \pm 0.007	0.919\pm0.002	0.925\pm0.003
boston	LN	0.590	0.264 \pm 0.034	0.000 \pm 0.079	0.533\pm0.036	0.397 \pm 0.000	0.529 \pm 0.028	0.409 \pm 0.015	0.525 \pm 0.035	0.575\pm0.011
	RF	0.662	0.129 \pm 0.015	0.124 \pm 0.068	0.658\pm0.025	0.281 \pm 0.001	0.584 \pm 0.006	0.439 \pm 0.096	0.597 \pm 0.038	0.694\pm0.041
	XGB	0.701	0.097 \pm 0.078	0.211 \pm 0.121	0.647\pm0.017	0.277 \pm 0.014	0.578 \pm 0.056	0.446 \pm 0.115	0.594 \pm 0.061	0.665\pm0.026
breast	LN	0.985	0.913 \pm 0.091	0.963 \pm 0.006	0.987\pm0.001	0.985 \pm 0.000	0.987\pm0.002	0.983 \pm 0.004	0.981 \pm 0.005	0.987\pm0.002
	RF	0.985	0.968 \pm 0.012	0.979 \pm 0.004	0.981\pm0.002	0.979 \pm 0.004	0.980\pm0.000	0.978 \pm 0.002	0.978 \pm 0.001	0.983\pm0.002
	XGB	0.984	0.958 \pm 0.025	0.970 \pm 0.009	0.987\pm0.001	0.982 \pm 0.002	0.982\pm0.002	0.982 \pm 0.002	0.982 \pm 0.002	0.983\pm0.003
credit	LN	0.836	0.538 \pm 0.093	0.500 \pm 0.000	0.780\pm0.017	0.665 \pm 0.000	0.801\pm0.006	0.773 \pm 0.038	0.816\pm0.020	0.755 \pm 0.011
	RF	0.837	0.505 \pm 0.097	0.500 \pm 0.000	0.791\pm0.007	0.722 \pm 0.014	0.820\pm0.010	0.763 \pm 0.019	0.781\pm0.026	0.741 \pm 0.027
	XGB	0.844	0.509 \pm 0.088	0.500 \pm 0.000	0.795\pm0.014	0.739 \pm 0.006	0.797\pm0.039	0.761 \pm 0.030	0.796\pm0.011	0.764 \pm 0.014
diabetes	LN	0.884	0.817 \pm 0.028	0.880 \pm 0.003	0.883\pm0.006	0.858 \pm 0.000	0.878 \pm 0.003	0.855 \pm 0.014	0.890\pm0.010	0.886\pm0.001
	RF	0.869	0.802 \pm 0.014	0.849 \pm 0.004	0.844\pm0.012	0.824 \pm 0.012	0.841 \pm 0.010	0.845 \pm 0.009	0.855\pm0.014	0.859\pm0.010
	XGB	0.867	0.811 \pm 0.005	0.851\pm0.001	0.847\pm0.009	0.831 \pm 0.003	0.849 \pm 0.010	0.840 \pm 0.009	0.852\pm0.015	0.848 \pm 0.017
iris	LN	1.000	0.272 \pm 0.068	0.996 \pm 0.006	0.999\pm0.002	0.985 \pm 0.000	0.983 \pm 0.015	1.000\pm0.000	0.971 \pm 0.018	0.997 \pm 0.005
	RF	1.000	0.396 \pm 0.099	0.992 \pm 0.012	1.000\pm0.000	1.000\pm0.000	0.993 \pm 0.005	0.993 \pm 0.005	0.999 \pm 0.002	0.988 \pm 0.017
	XGB	1.000	0.211 \pm 0.042	0.999 \pm 0.002	1.000\pm0.000	1.000\pm0.000	0.998 \pm 0.003	1.000\pm0.000	1.000\pm0.000	1.000\pm0.000
qsar	LN	0.906	0.716 \pm 0.085	0.669 \pm 0.120	0.867 \pm 0.012	0.673\pm0.000	0.880\pm0.003	0.887\pm0.005	0.874 \pm 0.013	0.876 \pm 0.006
	RF	0.936	0.648 \pm 0.036	0.666 \pm 0.117	0.882 \pm 0.006	0.616 \pm 0.009	0.907\pm0.007	0.880 \pm 0.008	0.873 \pm 0.006	0.884\pm0.004
	XGB	0.921	0.731 \pm 0.020	0.658 \pm 0.114	0.860 \pm 0.016	0.602 \pm 0.020	0.897\pm0.010	0.873 \pm 0.009	0.862 \pm 0.005	0.884\pm0.004
wdbc	LN	0.993	0.929 \pm 0.053	0.976 \pm 0.019	0.992\pm0.001	0.979 \pm 0.000	0.988\pm0.003	0.984 \pm 0.006	0.980 \pm 0.007	0.979 \pm 0.007
	RF	0.976	0.919 \pm 0.024	0.952 \pm 0.041	0.984\pm0.004	0.976 \pm 0.003	0.980 \pm 0.012	0.978 \pm 0.003	0.981\pm0.001	0.975 \pm 0.002
	XGB	0.990	0.930 \pm 0.021	0.949 \pm 0.035	0.986 \pm 0.002	0.973 \pm 0.003	0.988\pm0.002	0.982 \pm 0.004	0.987\pm0.003	0.985 \pm 0.006

Table 14: Comparison between different models in terms of time taken for training and generation. The values are in unit of seconds.

Dataset	Metric	CTAB+ [69]	TTVAE [59]	TabSyn [65]	FD [30]	GReaT [5]	RTF [55]	TabMT [22]	TabuLa [68]	TTF-S	TTF-L
adult	Train	787.379 \pm 3.334	194.718 \pm 0.085	1199.823 \pm 146.744	3857.698 \pm 10.002	10397.040 \pm 20.203	1875.904 \pm 34.663	6029.515 \pm 3.139	2859.160 \pm 6.888	1096.467 \pm 143.847	2503.830 \pm 564.922
	Generate	0.429 \pm 0.001	8.546 \pm 0.029	2.409 \pm 0.010	48.730 \pm 13.758	138.233 \pm 0.205	89.466 \pm 4.301	416.206 \pm 1.612	249.319 \pm 0.485	41.482 \pm 8.907	107.193 \pm 24.859
bank	Train	737.314 \pm 0.153	192.617 \pm 0.959	1865.473 \pm 418.666	4172.922 \pm 3.229	10295.769 \pm 1.720	835.167 \pm 1.619	7032.875 \pm 4.217	3079.641 \pm 2.237	1115.787 \pm 108.995	2551.349 \pm 724.774
	Generate	1.126 \pm 0.006	7.341 \pm 0.015	3.009 \pm 0.063	31.609 \pm 0.373	149.872 \pm 0.104	106.036 \pm 0.080	333.882 \pm 18.034	234.806 \pm 0.044	24.972 \pm 3.040	58.530 \pm 16.181
boston	Train	8.396	4.664 \pm 0.129	862.625 \pm 48.241	47.040 \pm 1.544	121.619 \pm 0.090	49.693 \pm 3.175	225.624 \pm 0.310	47.811 \pm 0.079	67.370 \pm 43.192	229.997 \pm 98.326
	Generate	0.083 \pm 0.001	0.172 \pm 0.029	0.156 \pm 0.003	0.447 \pm 0.007	2.422 \pm 0.006	3.059 \pm 0.006	2.524 \pm 0.001	3.012 \pm 0.013	0.533 \pm 0.028	1.560 \pm 0.401
breast	Train	8.479 \pm 0.026	6.355 \pm 0.592	1037.126 \pm 281.166	32.364 \pm 0.506	153.352 \pm 0.134	25.537 \pm 1.419	214.935 \pm 0.461	33.100 \pm 0.050	122.137 \pm 6.839	344.247 \pm 59.644
	Generate	0.056 \pm 0.008	0.144 \pm 0.032	0.249 \pm 0.003	0.771 \pm 0.005	3.434 \pm 0.016	0.759 \pm 0.003	1.653 \pm 0.013	6.652 \pm 0.011	0.620 \pm 0.033	1.463 \pm 0.208
credit	Train	8.400 \pm 0.033	12.288 \pm 2.809	726.006 \pm 67.662	185.868 \pm 5.293	277.555 \pm 0.388	63.648 \pm 0.758	703.238 \pm 1.755	78.538 \pm 0.338	179.304 \pm 56.926	458.389 \pm 89.990
	Generate	0.043 \pm 0.000	0.211 \pm 0.115	0.167 \pm 0.003	1.127 \pm 0.010	5.845 \pm 0.006	2.407 \pm 0.171	5.434 \pm 0.013	4.868 \pm 0.014	0.604 \pm 0.123	1.558 \pm 0.227
diabetes	Train	8.524 \pm 4.407	6.673 \pm 0.480	758.140 \pm 41.333	30.324 \pm 2.067	130.793 \pm 0.077	37.372 \pm 3.118	220.147 \pm 0.667	40.229 \pm 0.050	70.158 \pm 26.658	242.176 \pm 48.014
	Generate	0.047 \pm 0.001	0.064 \pm 0.001	0.139 \pm 0.000	0.383 \pm 0.000	1.496 \pm 0.000	1.504 \pm 0.007	0.786 \pm 0.006	3.994 \pm 0.007	0.343 \pm 0.062	1.169 \pm 0.364
iris	Train	7.267 \pm 0.021	2.489 \pm 0.005	620.864 \pm 35.603	5.055 \pm 1.403	24.975 \pm 0.018	15.369 \pm 1.242	32.846 \pm 0.011	-	86.143 \pm 41.970	126.315 \pm 29.440
	Generate	0.033 \pm 0.006	0.025 \pm 0.002	0.098 \pm 0.002	0.095 \pm 0.002	0.360 \pm 0.015	0.225 \pm 0.001	0.122 \pm 0.031	0.209 \pm 0.065	0.483 \pm 0.078	-
qsar	Train	18.389 \pm 0.217	13.144 \pm 1.576	694.890 \pm 76.480	664.578 \pm 3.603	566.658 \pm 23.451	152.950 \pm 0.819	1723.824 \pm 2.596	188.475 \pm 0.374	81.433 \pm 14.458	334.639 \pm 74.700
	Generate	0.206 \pm 0.006	0.432 \pm 0.006	0.336 \pm 0.005	2.608 \pm 0.007	46.712 \pm 3.062	10.997 \pm 0.072	23.723 \pm 0.025	20.261 \pm 5.972	1.270 \pm 0.094	4.118 \pm 0.606
wdbc	Train	10.795 \pm 0.089	8.168 \pm 0.171	631.546 \pm 68.070	306.120 \pm 3.189	265.340 \pm 2.411	183.908 \pm 1.047	643.120 \pm 1.028	-	31.884 \pm 4.836	169.320 \pm 54.606
	Generate	0.159 \pm 0.001	0.254 \pm 0.001	0.276 \pm 0.005	1.267 \pm 0.023	65.821 \pm 1.106	9.936 \pm 0.017	13.893 \pm 0.068	0.585 \pm 0.010	1.38	

transformer backbone flexibly configurable, and any modern or future more powerful versions of transformers can be substituted in.

Optimizing tree-based model. TabTreeFormer uses LightGBM fitted on the target column to introduce tabular inductive biases from tree-based models. While this is effective and easy to implement, modified tree-based models catered for guiding the generation may further improve the performance, such as using trees from a generative tree-based model (e.g. ARF), and selecting a better target column using some heuristics.

Smoothing quantized values. The dual-quantization tokenization may be further optimized with some sampling around the quantile values if use case requires smoother values in continuous values. Adapted ordinal embeddings with continuous raw values as additional input can also be applied. In this paper, we want to focus on showing the effectiveness of quantization and methods to handle quantized values. We leave the integration of raw continuous values on top of these methods for future works, as performance without raw continuous values is readily outstanding. Moreover, using quantized values only makes it much easier to change the backbone transformer.

Masked vs. Auto-regressive transformers. TabMT has demonstrated the effectiveness of a masked transformer with iterative decoding for tabular data generation, but TabMT does not provide ablation study result on masked vs. auto-regressive transformers. Thus, this approach may be used in place of a causal language model to further improve synthetic data quality. Further exploration could be interesting. In this paper, we want to focus on the most intuitive and simple usage of generative transformers, namely, auto-regressive generation, as the performance of this simple case is readily outstanding. Moreover, using the standard auto-regressive setting makes it much easier to integrate with other training optimizations available on open-source seq2seq trainers (e.g., Hugging Face).

G Broader Impact

Extension to general tabular tasks. The idea of introducing tree-based models to transformers on tabular data may not be limited to generation tasks, but also applies to tasks like classification and regression. We envision tabular models designed for other tasks inspired by TabTreeFormer’s design of the integration of a tree-based model to transformer would improve its performance by taking the advantage of both.

General ordinal token space learning. The proposed methods to learn the ordinal token space, including the embedding and loss, can be applied to any other task involving ordinal tokens, especially when the ordinal tokens’ relation is absolute and monotonic instead of relative and non-periodic.

NeurIPS Paper Checklist

1. Claims

Question: Do the main claims made in the abstract and introduction accurately reflect the paper's contributions and scope?

Answer: [\[Yes\]](#)

Justification: We provide our algorithm contribution in Section 3. Detailed theoretical proofs are provided in the Appendix. Experimental results that supports our improvement claim are provided in Section 4.

Guidelines:

- The answer NA means that the abstract and introduction do not include the claims made in the paper.
- The abstract and/or introduction should clearly state the claims made, including the contributions made in the paper and important assumptions and limitations. A No or NA answer to this question will not be perceived well by the reviewers.
- The claims made should match theoretical and experimental results, and reflect how much the results can be expected to generalize to other settings.
- It is fine to include aspirational goals as motivation as long as it is clear that these goals are not attained by the paper.

2. Limitations

Question: Does the paper discuss the limitations of the work performed by the authors?

Answer: [\[Yes\]](#)

Justification: For our algorithm design, limitations and future work are discussed in Appendix F. For broader challenges in generative model design for tabular data synthesis, in Section 4, through the experimental results, we show the trade-off between the utility and privacy. A more detailed discussion on utility and privacy dilemma is provided in Appendix E.2.

Guidelines:

- The answer NA means that the paper has no limitation while the answer No means that the paper has limitations, but those are not discussed in the paper.
- The authors are encouraged to create a separate "Limitations" section in their paper.
- The paper should point out any strong assumptions and how robust the results are to violations of these assumptions (e.g., independence assumptions, noiseless settings, model well-specification, asymptotic approximations only holding locally). The authors should reflect on how these assumptions might be violated in practice and what the implications would be.
- The authors should reflect on the scope of the claims made, e.g., if the approach was only tested on a few datasets or with a few runs. In general, empirical results often depend on implicit assumptions, which should be articulated.
- The authors should reflect on the factors that influence the performance of the approach. For example, a facial recognition algorithm may perform poorly when image resolution is low or images are taken in low lighting. Or a speech-to-text system might not be used reliably to provide closed captions for online lectures because it fails to handle technical jargon.
- The authors should discuss the computational efficiency of the proposed algorithms and how they scale with dataset size.
- If applicable, the authors should discuss possible limitations of their approach to address problems of privacy and fairness.
- While the authors might fear that complete honesty about limitations might be used by reviewers as grounds for rejection, a worse outcome might be that reviewers discover limitations that aren't acknowledged in the paper. The authors should use their best judgment and recognize that individual actions in favor of transparency play an important role in developing norms that preserve the integrity of the community. Reviewers will be specifically instructed to not penalize honesty concerning limitations.

3. Theory assumptions and proofs

Question: For each theoretical result, does the paper provide the full set of assumptions and a complete (and correct) proof?

Answer: [\[Yes\]](#)

Justification: We provide 3 theorems and 1 lemma in our paper. Except the Theorem 1 which is easy to prove, we provide detailed theoretical proofs for the rest of Theorems and Lemma in Appendix B.5, Appendix C.1 and Appendix C.2.

Guidelines:

- The answer NA means that the paper does not include theoretical results.
- All the theorems, formulas, and proofs in the paper should be numbered and cross-referenced.
- All assumptions should be clearly stated or referenced in the statement of any theorems.
- The proofs can either appear in the main paper or the supplemental material, but if they appear in the supplemental material, the authors are encouraged to provide a short proof sketch to provide intuition.
- Inversely, any informal proof provided in the core of the paper should be complemented by formal proofs provided in appendix or supplemental material.
- Theorems and Lemmas that the proof relies upon should be properly referenced.

4. Experimental result reproducibility

Question: Does the paper fully disclose all the information needed to reproduce the main experimental results of the paper to the extent that it affects the main claims and/or conclusions of the paper (regardless of whether the code and data are provided or not)?

Answer: **[Yes]**

Justification: This information is provided in Section 4, Appendix A and Appendix D.1.

Guidelines:

- The answer NA means that the paper does not include experiments.
- If the paper includes experiments, a No answer to this question will not be perceived well by the reviewers: Making the paper reproducible is important, regardless of whether the code and data are provided or not.
- If the contribution is a dataset and/or model, the authors should describe the steps taken to make their results reproducible or verifiable.
- Depending on the contribution, reproducibility can be accomplished in various ways. For example, if the contribution is a novel architecture, describing the architecture fully might suffice, or if the contribution is a specific model and empirical evaluation, it may be necessary to either make it possible for others to replicate the model with the same dataset, or provide access to the model. In general, releasing code and data is often one good way to accomplish this, but reproducibility can also be provided via detailed instructions for how to replicate the results, access to a hosted model (e.g., in the case of a large language model), releasing of a model checkpoint, or other means that are appropriate to the research performed.
- While NeurIPS does not require releasing code, the conference does require all submissions to provide some reasonable avenue for reproducibility, which may depend on the nature of the contribution. For example
 - (a) If the contribution is primarily a new algorithm, the paper should make it clear how to reproduce that algorithm.
 - (b) If the contribution is primarily a new model architecture, the paper should describe the architecture clearly and fully.
 - (c) If the contribution is a new model (e.g., a large language model), then there should either be a way to access this model for reproducing the results or a way to reproduce the model (e.g., with an open-source dataset or instructions for how to construct the dataset).
 - (d) We recognize that reproducibility may be tricky in some cases, in which case authors are welcome to describe the particular way they provide for reproducibility. In the case of closed-source models, it may be that access to the model is limited in some way (e.g., to registered users), but it should be possible for other researchers to have some path to reproducing or verifying the results.

5. Open access to data and code

Question: Does the paper provide open access to the data and code, with sufficient instructions to faithfully reproduce the main experimental results, as described in supplemental material?

Answer: **[Yes]**

Justification: The code is available via the link provided in the abstract. All datasets are sourced from OpenML; detailed loading instructions are provided in Appendix D.2.

Guidelines:

- The answer NA means that paper does not include experiments requiring code.
- Please see the NeurIPS code and data submission guidelines (<https://nips.cc/public/guides/CodeSubmissionPolicy>) for more details.
- While we encourage the release of code and data, we understand that this might not be possible, so “No” is an acceptable answer. Papers cannot be rejected simply for not including code, unless this is central to the contribution (e.g., for a new open-source benchmark).
- The instructions should contain the exact command and environment needed to run to reproduce the results. See the NeurIPS code and data submission guidelines (<https://nips.cc/public/guides/CodeSubmissionPolicy>) for more details.
- The authors should provide instructions on data access and preparation, including how to access the raw data, preprocessed data, intermediate data, and generated data, etc.
- The authors should provide scripts to reproduce all experimental results for the new proposed method and baselines. If only a subset of experiments are reproducible, they should state which ones are omitted from the script and why.
- At submission time, to preserve anonymity, the authors should release anonymized versions (if applicable).
- Providing as much information as possible in supplemental material (appended to the paper) is recommended, but including URLs to data and code is permitted.

6. Experimental setting/details

Question: Does the paper specify all the training and test details (e.g., data splits, hyper-parameters, how they were chosen, type of optimizer, etc.) necessary to understand the results?

Answer: [\[Yes\]](#)

Justification: This information is provided in Section 4, Appendix A and Appendix D.1.

Guidelines:

- The answer NA means that the paper does not include experiments.
- The experimental setting should be presented in the core of the paper to a level of detail that is necessary to appreciate the results and make sense of them.
- The full details can be provided either with the code, in appendix, or as supplemental material.

7. Experiment statistical significance

Question: Does the paper report error bars suitably and correctly defined or other appropriate information about the statistical significance of the experiments?

Answer: [\[Yes\]](#)

Justification: We repeated all our experiments 3 times, we report the result standard deviation in all the result tables.

Guidelines:

- The answer NA means that the paper does not include experiments.
- The authors should answer “Yes” if the results are accompanied by error bars, confidence intervals, or statistical significance tests, at least for the experiments that support the main claims of the paper.
- The factors of variability that the error bars are capturing should be clearly stated (for example, train/test split, initialization, random drawing of some parameter, or overall run with given experimental conditions).
- The method for calculating the error bars should be explained (closed form formula, call to a library function, bootstrap, etc.)
- The assumptions made should be given (e.g., Normally distributed errors).
- It should be clear whether the error bar is the standard deviation or the standard error of the mean.
- It is OK to report 1-sigma error bars, but one should state it. The authors should preferably report a 2-sigma error bar than state that they have a 96% CI, if the hypothesis of Normality of errors is not verified.
- For asymmetric distributions, the authors should be careful not to show in tables or figures symmetric error bars that would yield results that are out of range (e.g. negative error rates).
- If error bars are reported in tables or plots, The authors should explain in the text how they were calculated and reference the corresponding figures or tables in the text.

8. Experiments compute resources

Question: For each experiment, does the paper provide sufficient information on the computer resources (type of compute workers, memory, time of execution) needed to reproduce the experiments?

Answer: [Yes]

Justification: In Appendix D.1.

Guidelines:

- The answer NA means that the paper does not include experiments.
- The paper should indicate the type of compute workers CPU or GPU, internal cluster, or cloud provider, including relevant memory and storage.
- The paper should provide the amount of compute required for each of the individual experimental runs as well as estimate the total compute.
- The paper should disclose whether the full research project required more compute than the experiments reported in the paper (e.g., preliminary or failed experiments that didn't make it into the paper).

9. Code of ethics

Question: Does the research conducted in the paper conform, in every respect, with the NeurIPS Code of Ethics <https://neurips.cc/public/EthicsGuidelines>?

Answer: [Yes]

Justification: We reviewed it and comply with the code.

Guidelines:

- The answer NA means that the authors have not reviewed the NeurIPS Code of Ethics.
- If the authors answer No, they should explain the special circumstances that require a deviation from the Code of Ethics.
- The authors should make sure to preserve anonymity (e.g., if there is a special consideration due to laws or regulations in their jurisdiction).

10. Broader impacts

Question: Does the paper discuss both potential positive societal impacts and negative societal impacts of the work performed?

Answer: [Yes]

Justification: In Appendix G.

Guidelines:

- The answer NA means that there is no societal impact of the work performed.
- If the authors answer NA or No, they should explain why their work has no societal impact or why the paper does not address societal impact.
- Examples of negative societal impacts include potential malicious or unintended uses (e.g., disinformation, generating fake profiles, surveillance), fairness considerations (e.g., deployment of technologies that could make decisions that unfairly impact specific groups), privacy considerations, and security considerations.
- The conference expects that many papers will be foundational research and not tied to particular applications, let alone deployments. However, if there is a direct path to any negative applications, the authors should point it out. For example, it is legitimate to point out that an improvement in the quality of generative models could be used to generate deepfakes for disinformation. On the other hand, it is not needed to point out that a generic algorithm for optimizing neural networks could enable people to train models that generate Deepfakes faster.
- The authors should consider possible harms that could arise when the technology is being used as intended and functioning correctly, harms that could arise when the technology is being used as intended but gives incorrect results, and harms following from (intentional or unintentional) misuse of the technology.
- If there are negative societal impacts, the authors could also discuss possible mitigation strategies (e.g., gated release of models, providing defenses in addition to attacks, mechanisms for monitoring misuse, mechanisms to monitor how a system learns from feedback over time, improving the efficiency and accessibility of ML).

11. Safeguards

Question: Does the paper describe safeguards that have been put in place for responsible release of data or models that have a high risk for misuse (e.g., pretrained language models, image generators, or scraped datasets)?

Answer: [NA]

Justification:

Guidelines:

- The answer NA means that the paper poses no such risks.
- Released models that have a high risk for misuse or dual-use should be released with necessary safeguards to allow for controlled use of the model, for example by requiring that users adhere to usage guidelines or restrictions to access the model or implementing safety filters.
- Datasets that have been scraped from the Internet could pose safety risks. The authors should describe how they avoided releasing unsafe images.
- We recognize that providing effective safeguards is challenging, and many papers do not require this, but we encourage authors to take this into account and make a best faith effort.

12. Licenses for existing assets

Question: Are the creators or original owners of assets (e.g., code, data, models), used in the paper, properly credited and are the license and terms of use explicitly mentioned and properly respected?

Answer: [\[Yes\]](#)

Justification: We acknowledged the datasets we used are from OpenML in Section 4.

Guidelines:

- The answer NA means that the paper does not use existing assets.
- The authors should cite the original paper that produced the code package or dataset.
- The authors should state which version of the asset is used and, if possible, include a URL.
- The name of the license (e.g., CC-BY 4.0) should be included for each asset.
- For scraped data from a particular source (e.g., website), the copyright and terms of service of that source should be provided.
- If assets are released, the license, copyright information, and terms of use in the package should be provided. For popular datasets, paperswithcode.com/datasets has curated licenses for some datasets. Their licensing guide can help determine the license of a dataset.
- For existing datasets that are re-packaged, both the original license and the license of the derived asset (if it has changed) should be provided.
- If this information is not available online, the authors are encouraged to reach out to the asset's creators.

13. New assets

Question: Are new assets introduced in the paper well documented and is the documentation provided alongside the assets?

Answer: [\[Yes\]](#)

Justification: <https://anonymous.4open.science/r/tabtreeformer-9585>

Guidelines:

- The answer NA means that the paper does not release new assets.
- Researchers should communicate the details of the dataset/code/model as part of their submissions via structured templates. This includes details about training, license, limitations, etc.
- The paper should discuss whether and how consent was obtained from people whose asset is used.
- At submission time, remember to anonymize your assets (if applicable). You can either create an anonymized URL or include an anonymized zip file.

14. Crowdsourcing and research with human subjects

Question: For crowdsourcing experiments and research with human subjects, does the paper include the full text of instructions given to participants and screenshots, if applicable, as well as details about compensation (if any)?

Answer: [\[NA\]](#)

Justification:

Guidelines:

- The answer NA means that the paper does not involve crowdsourcing nor research with human subjects.

- Including this information in the supplemental material is fine, but if the main contribution of the paper involves human subjects, then as much detail as possible should be included in the main paper.
- According to the NeurIPS Code of Ethics, workers involved in data collection, curation, or other labor should be paid at least the minimum wage in the country of the data collector.

15. Institutional review board (IRB) approvals or equivalent for research with human subjects

Question: Does the paper describe potential risks incurred by study participants, whether such risks were disclosed to the subjects, and whether Institutional Review Board (IRB) approvals (or an equivalent approval/review based on the requirements of your country or institution) were obtained?

Answer: [NA]

Justification:

Guidelines:

- The answer NA means that the paper does not involve crowdsourcing nor research with human subjects.
- Depending on the country in which research is conducted, IRB approval (or equivalent) may be required for any human subjects research. If you obtained IRB approval, you should clearly state this in the paper.
- We recognize that the procedures for this may vary significantly between institutions and locations, and we expect authors to adhere to the NeurIPS Code of Ethics and the guidelines for their institution.
- For initial submissions, do not include any information that would break anonymity (if applicable), such as the institution conducting the review.

16. Declaration of LLM usage

Question: Does the paper describe the usage of LLMs if it is an important, original, or non-standard component of the core methods in this research? Note that if the LLM is used only for writing, editing, or formatting purposes and does not impact the core methodology, scientific rigorousness, or originality of the research, declaration is not required.

Answer: [NA]

Justification:

Guidelines:

- The answer NA means that the core method development in this research does not involve LLMs as any important, original, or non-standard components.
- Please refer to our LLM policy (<https://neurips.cc/Conferences/2025/LLM>) for what should or should not be described.